

AEDC-TR-70-215

cy 1

**ARCHIVE COPY  
DO NOT LOAN**

**INFRARED REFLECTANCE OF  
WATER FROSTS CONDENSED ON  
LIQUID-NITROGEN-COOLED SURFACES  
IN VACUUM**

**B. E. Wood, A. M. Smith, B. A. Seiber, et al.  
ARO, Inc.**

**December 1970**

This document has been approved for public release and sale; its distribution is unlimited.

**VON KÁRMÁN GAS DYNAMICS FACILITY  
ARNOLD ENGINEERING DEVELOPMENT CENTER  
AIR FORCE SYSTEMS COMMAND  
ARNOLD AIR FORCE STATION, TENNESSEE**

PROPERTY OF U S AIR FORCE  
AEDC LIBRARY  
F40600-71-C-0002

AEDC TECHNICAL LIBRARY



5 0720 0000 0210 5

# ***NOTICES***

When U. S. Government drawings specifications, or other data are used for any purpose other than a definitely related Government procurement operation, the Government thereby incurs no responsibility nor any obligation whatsoever, and the fact that the Government may have formulated, furnished, or in any way supplied the said drawings, specifications, or other data, is not to be regarded by implication or otherwise, or in any manner licensing the holder or any other person or corporation, or conveying any rights or permission to manufacture, use, or sell any patented invention that may in any way be related thereto.

Qualified users may obtain copies of this report from the Defense Documentation Center.

References to named commercial products in this report are not to be considered in any sense as an endorsement of the product by the United States Air Force or the Government.

**INFRARED REFLECTANCE OF  
WATER FROSTS CONDENSED ON  
LIQUID-NITROGEN-COOLED SURFACES  
IN VACUUM**

**B.E. Wood, A.M. Smith, B.A. Seiber, et al.  
ARO, Inc.**

This document has been approved for public release and  
sale: its distribution is unlimited.

## FOREWORD

The research reported herein was sponsored by Headquarters, Arnold Engineering Development Center (AEDC), Air Force Systems Command (AFSC), Arnold Air Force Station, Tennessee, under Program Element 61102F, Project 8951.

The results of the research were obtained by ARO, Inc. (a subsidiary of Sverdrup & Parcel and Associates, Inc.), contract operator of AEDC, AFSC, under Contract F40600-71-C-0002. The work was performed under ARO Projects No. SW5906 and SW5007 during the period from July 1968 through September 1969. The manuscript was submitted for publication on July 1, 1970.

J.A. Roux, University of Tennessee Space Institute, was also a co-author of this report.

This technical report has been reviewed and is approved.

Michael G. Buja  
First Lieutenant, USAF  
Research Division  
Directorate of Technology

Harry L. Maynard  
Colonel, USAF  
Director of Technology

**ABSTRACT**

Spectral absolute reflectance measurements from 0.5 to 12.0 $\mu$  were made for water cryodeposits formed on liquid-nitrogen-cooled surfaces in a vacuum infrared integrating sphere. The results are presented as functions of view angle, deposit thickness, and wavelength. The deposits were formed at pressures between  $2 \times 10^{-2}$  and  $4 \times 10^{-2}$  torr on cryogenically cooled black epoxy paint and polished stainless steel surfaces. All three forms of Ice I were observed - hexagonal, cubic, and amorphous or vitreous - and depended on the cryosurface temperature. The temperature of the deposit was found to play a strong role in determining the reflectance of any water deposit. From the results obtained in this investigation, important conclusions are drawn with regard to effects on space simulation and component studies in ground test facilities.

## CONTENTS

	<u>Page</u>
ABSTRACT . . . . .	iii
NOMENCLATURE . . . . .	vi
I. INTRODUCTION . . . . .	1
II. SURVEY OF WATER DEPOSIT FORMATION PROPERTIES . . . . .	2
III. APPARATUS . . . . .	3
IV. PROCEDURE . . . . .	4
V. RESULTS	
5.1 Black Epoxy Paint Substrate . . . . .	5
5.2 Stainless Steel Substrate . . . . .	8
VI. DISCUSSION . . . . .	10
VII. CONCLUDING REMARKS . . . . .	12
REFERENCES . . . . .	13

## APPENDIX ILLUSTRATIONS

### Figure

1. Infrared Integrating Sphere and Optical Systems . . . . .	17
2. Schematic of Infrared Integrating Sphere and Components . . . . .	18
3. Spectral Reflectance of Water Cryodeposits Formed on a Black Epoxy Painted Substrate . . . . .	19
4. Reflectance and Temperature Profile of Water Cryodeposit during Warmup . . . . .	21
5. Comparison of Reflectances of a 4-mm Water Deposit before and after Warmup . . . . .	22
6. Temperature versus Time Plot of a Water Deposit during Two Consecutive Warmups . . . . .	23
7. Dependence of Reflectance on View Angle, $\theta$ , for Water Deposits Formed on a Black Epoxy Painted Substrate . . . . .	24
8. Dependence of Reflectance on Deposit Thickness for Water Deposits Formed on a Black Epoxy Painted Substrate . . . . .	27
9. Reflectance versus Thickness of a Water Deposit Formed Continuously on a Black Epoxy Painted Substrate for $\lambda = 0.55\mu$ . . . . .	28
10. Comparison of Experimental and Analytical Results for Reflectance versus Thickness of Water Deposits Formed on a Black Epoxy Painted Substrate . . . . .	29
11. Spectral Reflectance of Water Cryodeposits Formed on a Polished Stainless Steel Substrate . . . . .	30
12. Comparison of Reflectances of a 4-mm Water Deposit on Stainless Steel before and after Warmup . . . . .	34
13. Reflectance versus Thickness of Water Cryodeposits Formed on a Polished Stainless Steel Substrate . . . . .	35

## NOMENCLATURE

$B_s(\theta, \lambda)$	Detector output obtained viewing the test surface
$B_w(\lambda)$	Detector output obtained viewing the sphere wall
$N_{H_2O}$	Refractive index of water
$N_{sub}$	Refractive index of substrate
$\theta$	View angle, deg
$\lambda$	Wavelength, $\mu$
$\mu$	Microns
$\rho$	Reflectance
$\tau$	Thickness
$\dot{\tau}$	Deposition rate

## SECTION I INTRODUCTION

It is understandable that a substance as common as water would have been the subject of many papers and reports. In many instances, however, the properties of water are not known, especially in the solid form. In the fields of space simulation, radiative transfer, sensor testing, and planetary environments, there are numerous reasons for interest in this solid form, either as ice, frost, or cryodeposit. In space simulation testing and sensor evaluation in ground test facilities, water as a frost or ice can be undesirable. The thermal radiative properties of a cryogenically cooled surface may change because of the cryopumping of gaseous water by the cold surfaces. Additionally, the frost properties such as reflectance, transmittance, and emittance are of interest with regard to calibration of low temperature blackbodies, and any experimental optical arrangement requiring cryogenically cooled mirrors, windows or lenses.

Much effort has been spent studying the properties of water (Ref. 1). Most of the emphasis has been placed on determining the absorption regions in the infrared for water substances in the gaseous, liquid, and solid phases. However, essentially nothing has been done for determining the absolute infrared reflectance of frosts or cryodeposits. The reasons for this are understandable and are due to the fact that: (1) the deposits often scatter a significant amount of radiation which makes collecting all the reflected energy difficult, (2) studies of high purity frosts require that the deposits be formed in vacuum, (3) absolute reflectance measurements, in general, require special care in the technique of measurement, and (4) since all reflected radiation must be collected or sampled, the design of the reflectance measurement apparatus is restricted to either an integrating sphere or to some type of  $2\pi$  steradian mirror.

Previous papers and reports have presented the spectral absolute reflectances of carbon dioxide cryodeposits in the infrared region from 0.5 to 12.0  $\mu$  (Refs. 2 and 3) and relative reflectance measurements in the region from 0.36 to 1.15  $\mu$  (Ref. 4). Spectral reflectance data have also been obtained in situ on water cryodeposits and were reported in Ref. 4. These were also restricted to the wavelength range from 0.36 to 1.15  $\mu$  and were relative to the reflectance of MgO. This investigation presents spectral absolute reflectance data for water cryodeposits in the wavelength range from 0.5 to 12.0  $\mu$ . The deposits, up to 4.0 mm thick, were formed on liquid-nitrogen-cooled stainless steel surfaces that were either polished or coated with a black epoxy paint.

Reflectance measurements on water cryodeposits, frost, and ice, heretofore, were either specular reflectance measurements, relative reflectance measurements, measurements at atmospheric conditions, or were data that simply gave an indication of the presence of absorption bands and structure without regard to the quantitative reflecting ability of the deposits.

In the present study an integrating sphere technique was used in which absolute reflectance measurements were made in the infrared, regardless of whether the deposit was a specular or a diffuse reflector. The infrared integrating sphere, which can be used for reflectance measurements out to at least 12  $\mu$ , has been discussed previously in Refs. 2 and 3.

The results of this investigation show that water deposit reflectances are strongly dependent on wavelength and on the manner in which the deposit is formed. The results are presented as functions of substrate material, view angle, wavelength, and deposit thickness. These results are discussed considering various cryogenic surface applications wherever possible. Since water vapor is much more abundant than carbon dioxide in the earth's atmosphere, it is the most important condensate on most cryogenic surfaces. Therefore, the reflectances of these surfaces, and water frosts in general, are of considerable interest.

## SECTION II SURVEY OF WATER DEPOSIT FORMATION PROPERTIES

Besides the high pressure forms of ice, there are three forms of ice which are formed at low pressures and designated as Ice I (Ref. 5). Ice I consists of two crystalline forms, hexagonal (Ih) and cubic (Ic), and a third form which is referred to as amorphous or vitreous and has no crystalline structure. The conditions for formation of these three types has been the subject of much discussion, and considerable data has been gathered by investigators and are summarized in tabular form in Ref. 6. For ice formed from the liquid at atmospheric pressure, only Ih has been observed. The general consensus obtained from the previous studies is that water deposits formed from the vapor on surfaces in vacuum, which are 115°K or colder, will be amorphous. If the surface is between approximately 115 and 150°K, the deposit will be Ic (Ref. 7). For surface temperatures higher than 150°K, the frosts formed will be Ih. It is also generally agreed that these temperatures of formation are not rigid. Hence, mixtures of the different forms can be obtained in the vicinity of the stated temperatures.

The temperatures stated previously are those of the surface while the vapor is condensing. Once formed, the deposit can also change structure, but only in a given direction. The deposit can go from amorphous to cubic to hexagonal, but the processes are not reversible. The most conclusive method for studying these changes in crystalline form is through X-ray diffraction techniques such as that used by Dowell and Rinfret (Ref. 7). They observed that if the deposit is warmed at a fairly high rate, that is, 5°C/min., the amorphous to cubic transition would be observed in the vicinity of 145°K. These findings agree with the work of Pryde and Jones (Ref. 8) and also that of this study. Dowell and Rinfret also show that the conversion of amorphous to cubic can occur at lower temperatures but requires longer time periods. Therefore, for lower warmup rates, the transition can be gradual between 115 and 150°K or a sudden jump may occur as the surface is warmed. Dowell and Rinfret also state that no further transformation change is seen until the temperature reaches 200°K, whereupon Ic begins to transform to Ih. This agrees with the earlier findings of Burton and Oliver (Ref. 9) but disagrees with Bertie et al. (Ref. 10). In Ref. 10 the Ic to Ih transition was reported to occur at about 170°K, but, as they point out, the transition temperature depends to a considerable extent on the history of the deposit.

The amorphous to Ic transition for water deposits is an exothermic reaction. There is a sudden increase in temperature from about 145°K up to approximately 165°K within seconds if the warmup rate is 5°C/min. or greater. The heat of crystallization for

this transformation has also been studied by several investigators. Published values ranging from 2 to 24 cal/gm have been reported with values from 6 to 12 cal/gm being the most common. The variation in these values again could be due to the warmup rate and, also, to possible contamination of the amorphous ice by some of the cubic form. Either factor could lower the observed heat of crystallization. During the cubic to hexagonal transformation, only small amounts of heat release have been observed. Essentially, all investigators are in agreement on this point.

While there is considerable variation in the results, there is also considerable variation in the experimental conditions under which these deposits were studied. Parameters which must be considered are the pressure during formation, the rate of formation, the deposit thickness, the heat capacity of the substance on which the deposits are formed, and the technique and location of temperature measurement. These factors can affect the determination of the local temperature of the deposit. The temperature of the condensing surface has already been established as probably the one most important parameter in determining the form of the condensed deposit.

Infrared absorption spectra of the two crystalline forms of Ice I have been studied by Ockman (Ref. 11), Bertie and Whalley (Ref. 12), and Hornig, White, and Reding (Ref. 13). No significant differences were seen in the absorption spectra of the two forms. This means that the location of the major absorption bands occurs in the same vicinity for both Ih and Ic. Kieffer (Ref. 14), reports spectral "reflectance" measurements on vitreous ice out to  $3.2 \mu$ . However, indications are that his deposits were crystalline rather than amorphous. First of all, his deposits were formed at pressures of 3 torr which in most cases is too high to obtain amorphous ice. He also reports data obtained for fine and coarse grain deposits which seem inconsistent with the physical appearance of glassy amorphous ice. Finally, he states that the visual albedo was at least 50 percent for a deposit thickness of only  $1.0 \mu$  ( $1.0 \text{ mg/sq-cm}$ ). The last point is particularly doubtful since thin amorphous deposits are glassy and essentially transparent to the eye. Therefore, until the present study, there have been no established data available on the spectral infrared reflectance of amorphous ice.

### SECTION III APPARATUS

The infrared integrating sphere system (see Figs. 1 and 2) has been previously discussed in detail in Refs. 2 and 3. Absolute hemispherical-angular reflectance measurements were obtained in vacuum using a powdered sodium chloride coated integrating sphere. The pumping system consisted of an ion pump and a liquid-nitrogen-trapped 4-in. diffusion pump backed by a mechanical pump. Pressures in the  $10^{-7}$  torr range were routinely achieved. Chamber pressures were monitored using a thermocouple gage and an ion gage.

The cryosurface was a hollow, stainless steel, rectangular block of dimensions 1 by 1-1/2 by 1/2 in. which could be cooled by continuously flowing liquid nitrogen through it. The test surface was one of the 1-by 1-1/2-in. faces and was either polished stainless steel or coated with black epoxy paint. A copper-constantan thermocouple was silver

soldered to the surface for monitoring the test surface temperature. To restrict the cryopumping area to only that of the cryosurface, the liquid-nitrogen supply lines inside the vacuum chamber were vacuum jacketed. A guard was attached at one end to the vacuum jacket with the other end closely surrounding, but not touching, the junction of the vacuum jacket with the cryosurface. This eliminated any pumping on the lower portion of the vacuum jacket stem. With this arrangement the pumping area was 32.6 sq cm. The test surface assembly and liquid-nitrogen transfer lines could be rotated without disturbing the vacuum. This allowed reflectance measurements to be made as a function of view angle from 0 to 60 deg, as measured from the test surface normal.

The optical transfer, source, and detection systems were the same as those described in Ref. 3. Radiation from a 1000-w tungsten-halogen lamp was chopped at 13 Hz and focused on the sphere wall (see Fig. 2). Radiation reflected from either the test surface or sphere wall was focused on the entrance slit of a single pass monochromator which had an NaCl prism as the dispersing element. The radiation was detected by a Reeder<sup>®</sup> thermocouple and the output amplified, synchronously rectified, and displayed on a strip chart recorder.

A gas addition system was used to introduce water vapor into the sphere to be cryopumped. Prior to flow of the water vapor into the sphere, the distilled water was boiled under vacuum while being pumped with a mechanical pump to remove gases absorbed in the water. The mass flow rate of the water vapor through a rotameter was calibrated by weighing an evacuated glass flask, cooling it with liquid nitrogen, and allowing the vapor to condense in the flask. After about 10 minutes of flow, the flask was again weighed on a balance which was accurate to better than  $10^{-3}$  gm. Knowing the total mass deposited and the flow time, the mass flow rate  $\dot{m}$  was determined. This was found to be a very good calibration technique with reproducibility being within  $\pm 1$  percent. For all experiments reported herein, a mass flow rate of  $2.18 \times 10^{-3}$  gm/sec was used which yielded a deposition rate of 0.24 gm/sq-cm hr.

#### SECTION IV PROCEDURE

Prior to the cryodeposit reflectance measurements, the infrared integrating sphere system was pumped down to approximately  $5 \times 10^{-7}$  torr, and reflectance measurements were made on the warm, bare, test surface, that is, on either the black epoxy paint surfaces or the polished stainless steel surfaces. Measurements were obtained using the hemispherical-angular technique which has been described previously in Refs. 2 and 3. Briefly, radiation from an external source was focused on the NaCl-coated wall of the sphere after passing through an NaCl window. The radiation was diffusely reflected by the salt coating throughout the sphere so that the sphere wall was uniformly illuminated. This caused the test surface to be uniformly and hemispherically irradiated. The procedure was to first obtain a detector output  $B_s(\theta, \lambda)$  by viewing the test surface at an angle  $\theta$  with respect to the surface normal. The wall of the sphere was then viewed similarly for the same wavelength and another detector output  $B_w(\lambda)$  recorded. The absolute reflectance was then determined from  $\rho = B_s(\theta, \lambda)/B_w(\lambda)$ . The important point for absolute reflectance measurements in the integrating sphere is that the area of the sphere wall viewed by the spectrometer is irradiated by the first reflection from the sphere wall, whereas the test surface is not.

After obtaining the warm, bare, test surface reflectance, liquid nitrogen was used to cool the test surface to an equilibrium temperature of 93°K. After valving off the integrating sphere from the pumping system, the water vapor flow into the sphere was started and the water condensed on the liquid-nitrogen-cooled surface. By allowing the gas to condense only on the cryosurface, a given flow time resulted in a certain deposit thickness. This could be calculated by knowing the mass flow rate, cryosurface pumping area, and density of deposit. The density of amorphous water cryodeposits has been reported to be 0.81 gm/cu-cm in Ref. 15. The deposits in this study were also amorphous and were formed under similar conditions to those stated in Ref. 15. Therefore, a density of 0.81 gm/cu-cm was used in calculating all deposit thicknesses. In order to ensure that these thicknesses were correct, deposits up to 150  $\mu$  thick were checked optically using thin-film interference techniques with a helium-neon laser as light source. The thicknesses determined by these two independent techniques were in good agreement and indicated that the density used in the calculations was correct.

After each thickness of deposit had been formed, reflectance measurements were made as a function of wavelength from 0.5 to 12.0  $\mu$  using the procedure discussed previously. Upon completion of reflectance measurements for a given thickness, the flow of water vapor was again started. The pressures during deposition remained relatively constant, ranging from  $1 \times 10^{-2}$  to  $4 \times 10^{-2}$  torr for the full range of thicknesses. This deposition pressure was an order of magnitude less than that for the water deposits formed and measured in Ref. 4. The temperature of the test surface prior to any deposition was about 93°K. During the time of deposit formation, the temperature would rise about 2 to 3°K. For increasing deposit thickness, the temperature also gradually increased with the final deposit thickness (4 mm) being formed at temperatures of approximately 103 to 106°K. As will be discussed later, this final temperature may have had some effect on the structure of the thick deposit.

After the final thickness (4 mm) of the deposit had been formed and the reflectance measured, the liquid-nitrogen flow to the surface was shut off. The reflectance was monitored at a given wavelength (0.55  $\mu$ ) as the temperature of the test surface increased. In this manner, crystallization effects were studied. In some cases the deposits were cooled back down to about 100°K and warmup effects again observed. Thereafter, the system was brought up to atmospheric pressure, the test surface withdrawn, and the final deposit thickness checked by means of a calibrated probe. Although thicknesses with this technique could not be determined more accurately than 0.5 mm, this was sufficient to show agreement with the previously mentioned methods of thickness determination. Indications were that the density did not vary appreciably with thickness and that the thickness appeared to be quite uniform over the entire surface.

## SECTION V RESULTS

### 5.1 BLACK EPOXY PAINT SUBSTRATE

Black epoxy paint was of most interest with regard to effects of water cryodeposits on the reflectance of space simulation chamber walls. The reflectance of the bare paint prior to cooldown was measured to be 5 percent or less for wavelengths less

than  $8 \mu$  (Fig. 3a). Between  $8$  and  $12 \mu$  there was a rise in reflectance up to  $8$  to  $8.5$  percent. When the surface was cooled with liquid nitrogen, it was observed that the reflectance in this region was reduced from  $8$  percent down to about  $3$  percent. For wavelengths less than  $8 \mu$  the reflectance was also decreased, but only by  $1$  or  $2$  percent.

Figures 3b through i are for the black substrate with water deposit thicknesses ranging from a relatively thin deposit,  $63 \mu$  ( $0.063$  mm) up to a relatively thick deposit ( $4.0$  mm). The pressure during deposition varied from  $2.5 \times 10^{-2}$  torr for the  $0.063$ -mm-thick deposit to  $4.0 \times 10^{-2}$  torr for the  $4$ -mm-thick deposit, so there was little dependence of pressure on thickness. The mass flow rate of the water vapor was  $2.18 \times 10^{-3}$  gm/sec, which gave a thickness deposition rate of  $0.825 \mu$ /sec.

The reflectance of the  $63\text{-}\mu$ -thick deposit was less than that of the bare paint surface at all wavelengths. In the visible region ( $0.5$  to  $0.7 \mu$ ), the reflectance was reduced from about  $4.5$  percent down to  $2.0$  percent and the reductions were even greater in the infrared ( $\lambda > 1.0 \mu$ ). For the thicker deposits, the reflectance increased steadily for wavelengths less than  $1.5 \mu$ . This wavelength seems to have been an abrupt cutoff point, since the reflectance at the longer wavelengths remained essentially constant at thicknesses from  $0.063$  to  $4.0$  mm. In contrast, the data for a thickness of  $4.0$  mm (Fig. 3h) showed the reflectance at  $0.5 \mu$  to be about  $47$  percent. In other experiments, the reflectance of the  $4$ -mm-thick deposits at  $0.5 \mu$  varied between  $43$  and  $50$  percent.

The increase in reflectance at the shorter wavelengths was attributable to scattering and, as would be expected, was highly wavelength dependent. For the  $1.0$ - and  $2.0$ -mm-thick deposits (Figs. 3f and g), the reflectance increased linearly with decreasing wavelength below about  $1.5 \mu$ . To the eye, the thicker deposits ( $1.0$  to  $4.0$  mm) had a slight, milky-white translucent appearance, whereas the thinner deposits ( $0.25$  mm and less) could not be detected visually. Since the thicker deposits did appear somewhat white, they may have been partially crystalline. In general, the deposits could be assumed to be amorphous. This will be discussed in greater detail later. The reflectance of the  $4$ -mm deposit showed a weak absorption band at  $1.04 \mu$  (Fig. 3h).

The data for all of the water deposit thicknesses  $\geq 0.125$  mm show a slight increase in reflectance in the wavelength region between  $3.1$  and  $3.25 \mu$ . This increase was caused by the anomalous dispersion effect which was observed earlier for carbon dioxide and discussed in Ref. 3. The effect was caused by the increase in refractive index at an absorption band. Otherwise, in the infrared, the reflectance was essentially independent of thickness and wavelength for  $\lambda > 1.5 \mu$ . Even for the largest thickness, when the effects of scattering would be expected to be greatest, the reflectance was still well below that obtained for the bare substrate. In the infrared, the general trend for water deposits formed on liquid-nitrogen-cooled substrates will be to make black surfaces blacker. This point presents interesting implications with regard to ground testing techniques and will be discussed later.

After the reflectance measurements were completed for the deposits in Figs. 3b through h, the liquid-nitrogen flow was turned off and the test surface allowed to warm up. As it warmed, both the cryosurface temperature and the reflectance at a wavelength

of  $0.55 \mu$  were monitored. These data are shown in Fig. 4. During the time of warmup the radiation source was still operating, since it was required for the reflectance measurements. The heat load from the radiation source caused the cryosurface to warm up at a fairly high rate of about  $15^\circ\text{K}/\text{min}$ . The reflectance stayed constant until a temperature of about  $145^\circ\text{K}$  was reached. At this point, there was a rapid increase in both the reflectance and temperature of the deposit. This is characteristic of transformations from the amorphous to cubic structure (Ref. 5). Further warming caused a steady rise in reflectance and temperature until at  $233^\circ\text{K}$  the reflectance leveled off at a value of 85 percent. After the test surface reached  $233^\circ\text{K}$ , the surface was again cooled with liquid nitrogen to approximately  $100^\circ\text{K}$ , and the spectral reflectance measured from  $0.5$  to  $12.0 \mu$ . The resulting spectral reflectance, shown in Fig. 5, was greater by a factor of about 2 over that observed for the deposit before warmup (Fig. 3h). With the increased scattering by the deposit, the absorption bands showed up more clearly at  $1.04$ ,  $1.25$ ,  $1.55$ ,  $2.03$ , and in the vicinity of  $2.85$  to  $3.25 \mu$ . Substantial scattering was also seen for the longer wavelengths up to  $12.0 \mu$ . This indicates that the effective size of the scattering centers was increased significantly.

After the spectral reflectance measurements shown in Fig. 5 were completed, the test surface was again allowed to warm up. However, no abrupt changes in temperature or reflectance were observed. Therefore, the structural changes are irreversible, at least for periods of a few hours. The change in reflectance is caused by the deposit, which originally is in a predominantly amorphous state, changing to the cubic crystalline state. This is an exothermic process as indicated by the sudden jump in temperature at  $145^\circ\text{K}$  in Fig. 4. After warmup to  $230^\circ\text{K}$  the final state is undoubtedly hexagonal. The gradual increase in reflectance seen in Fig. 4, for temperatures beyond  $175^\circ\text{K}$ , is probably due to the relatively slow conversion of the cubic to hexagonal on the outer portion of the deposit. The conversion proceeds inward as the temperature of the deposit increases. In one experiment the 4-mm-thick deposit was warmed up to about  $234^\circ\text{K}$ , cooled back down to  $100^\circ\text{K}$ , and then again warmed up (see Fig. 6). No structural change in the vicinity of  $145^\circ\text{K}$  was seen for the second warmup. This was true for several deposits when the temperature during a second warmup was monitored. The exothermic phase change establishes that amorphous ice was formed in these studies. Therefore, the conclusion of Beaumont, et al. (Ref. 16), who reported that amorphous ice could not be formed at deposition rates greater than  $0.01 \text{ gm}/\text{sq-cm hr}$  is in disagreement with the present results. The deposition rate for this study was  $0.24 \text{ gm}/\text{sq-cm hr}$ . Although the deposition rate is undoubtedly important, the cryogenic cooling capacity of the surface must also be considered. The ability to keep the equilibrium temperature of the depositing surface below about  $110^\circ\text{K}$ , regardless of flow rate or pressure, is probably the one controlling factor in obtaining amorphous ice.

The reflectance data reported in Fig. 3 were taken for  $\theta = 10 \text{ deg}$ . To determine the effect of varying  $\theta$ , reflectance measurements were made at angles from  $0$  to  $60 \text{ deg}$  and at wavelengths of  $0.5$ ,  $1.0$ ,  $2.0$ ,  $4.0$ , and  $8.0 \mu$  (Fig. 7). For the  $0.5$ -,  $1.0$ -, and  $2.0$ - $\mu$  data, the curves labeled 4\*mm are for a deposit which was (1) 4 mm thick, (2) warmed to  $220^\circ\text{K}$ , and (3) then recooled to  $100^\circ\text{K}$ . Any effect on the density and thickness of the deposit caused by the warmup is unknown. As seen in Fig. 7, there are no major variations with view angle and the curves follow the general shapes expected for reflectances of smooth dielectric surfaces.

The change in water reflectance with deposit thickness is shown in Fig. 8 for the wavelengths of 0.5, 1.0, 2.0, 4.0, and 8.0  $\mu$ . These data were obtained in an additional experiment as can be seen by the fact that the reflectance for the 4-mm-thick deposit in Fig. 8 for  $\lambda = 0.5 \mu$  is 3 to 4 percent less than for the corresponding thickness and wavelength shown in Fig. 3h. Figure 8 shows the gradual increase in reflectance with thickness for the 0.5 and 1.0  $\mu$  curves. For the other three wavelengths shown, the reflectance is largely independent (within 5 percent) of both thickness and wavelength.

The data shown in Fig. 8 were for deposits that were formed in layers rather than continuously. Figure 9 shows a continuous plot of the reflectance with thickness for the single wavelength, 0.55  $\mu$ . Although there is only a slight change in the curve shape around 2.4-mm thickness, it is enough to indicate a possible structure change. At 2.0-mm thickness the reflectance curve appears to have reached a plateau but then begins to rise again at a thickness of about 2.4 mm. The final reflectance of about 43 percent, however, agrees with the 44-percent value for 0.55  $\mu$  for the 4-mm-thick deposit shown in Fig. 3h. It is also near to the 43-percent value for the 0.5-micron curve shown in Fig. 8. Therefore, according to these results there are no significant differences in the reflectance of deposits formed continuously (Fig. 9) or in layers (Figs. 3h and 8).

In Ref. 3 a brief description of an analytical model was presented for determining the reflectance of isotropic absorbing and scattering media. In order to apply this model to the data shown in Fig. 8, the black surface was assumed to be diffusely reflecting and the surface of the deposit was assumed to be specular. With these assumptions, the model was used to predict the reflectances at various thicknesses after determining the absorption ( $k$ ) and scattering ( $\sigma$ ) coefficients using the reflectance at two thicknesses. As pointed out earlier, these deposits were predominantly amorphous so the scattering coefficient would be expected to be considerably lower than that for most water frosts. For  $\lambda = 0.5 \mu$  the values obtained were 12.48  $\text{cm}^{-1}$  for  $\sigma$  and 0.984  $\text{cm}^{-1}$  for  $k$ . It is important to point out that the absorption and scattering coefficients determined are valid for only this one deposit. This is due to the many factors which can influence the formations of water deposits as mentioned earlier. The analytical and experimental results are compared in Fig. 10. The agreement is good for deposits 2 mm thick and less. For the 4.0-mm-thick deposit the reflectance determined experimentally is about 5 percent higher than the analytical prediction. The good agreement for the smaller thicknesses indicates that the deposit is homogeneous, and the disagreement for the largest thickness suggests that the outer layer of the 4-mm-thick deposit was slightly more reflecting than the inner 2 mm. It is speculated that the outer layer was more reflecting as a result of being partially Ic. From the reflectance versus thickness curve shown in Fig. 9 this would seem very likely. Since the thick deposits did appear somewhat white, they were presumably at least partially cubic crystalline. The only other possible explanation for this appearance would be the presence of voids throughout the deposit which would serve as scattering centers.

## 5.2 STAINLESS STEEL SUBSTRATE

To study the dependence of reflectance on substrate, water deposits were also formed on the liquid-nitrogen-cooled polished stainless steel surface. This was the same test surface used previously but with the paint removed and the surface repolished. The

reflectance of the bare surface prior to cooldown is shown in Fig. 11a. For the thinnest deposit studied,  $30\ \mu$  (0.030 mm), the reflectance was reduced significantly (Fig. 11a). For this particular deposit thickness, absorption bands occurred at  $1.55\ \mu$ ,  $2.0\ \mu$ , a broad absorption around  $3.0\ \mu$ , and an absorption band centered at  $4.5\ \mu$ . For wavelengths between 5 and  $12\ \mu$  the deposit absorbed strongly for all wavelengths but did show slight peaks in the reflectance in the vicinity of  $8.0$ ,  $8.75$ , and  $9.6\ \mu$ . Regions of maximum transmission through the deposit were at about  $3.70$  and  $5.1\ \mu$  and also for most wavelengths below  $2.5\ \mu$ . The peak at  $3.7\ \mu$  also corresponds to a window in the transmission in the gaseous phase of water. For thicker deposits, the peak at  $3.7\ \mu$  quickly disappeared and the reflectance decreased for all wavelengths (Figs. 11b through g). The edge of strongest absorption moved from  $3.0\ \mu$  in Fig. 11b to  $1.5\ \mu$  in Fig. 11g. In the visible and near infrared, the reflectance dropped to about 30 percent for 0.25- and 0.50-mm-thick deposits. At these thicknesses, the surface usually appeared tannish-brown in color. Further increase in deposit thickness caused the visible and near infrared reflectance to increase. Finally, for a deposit thickness of 4.0 mm (Fig. 11g) the reflectance spectra looked very similar to that for the 4.0-mm-thick deposit on the black substrate (Fig. 3h). The main difference was that the reflectance in the infrared appeared to be about 5 percent higher for the deposits formed on the stainless steel substrate.

After the reflectance measurements were completed, the chamber was brought up to 740-mm pressure with dry nitrogen while the reflectance at  $0.55\ \mu$  was monitored to check pressure effects. Although the liquid-nitrogen flow through the test surface was continued, the temperature increased from about 100 up to  $115^\circ\text{K}$ . During this pressurization there also was a gradual increase in deposit reflectance from the initial value of 46 percent. After about an hour, the reflectance had risen to about 65 percent and was probably caused by the warming effect of the surrounding gas on the outer portion of the deposit. The test surface temperature was  $115^\circ\text{K}$  which was considerably less than the transition temperature of  $145^\circ\text{K}$  observed earlier. However, because of the high heat load from the light source, the outer portion of the frost may have reached sufficiently high temperatures to have caused the phase transition from the amorphous to the cubic state. The transition would have begun on the outer surface and advanced slowly inward with time. Also, Dowell and Rinfret (Ref. 7) have shown that amorphous ice will change to cubic for any temperature between 113 and  $145^\circ\text{K}$  with the deposits at the colder temperatures requiring much longer times to transform.

After the deposit reflectance had reached 65 percent the chamber was then evacuated to approximately  $10^{-4}$  torr. The liquid nitrogen was turned off to allow the cryosurface to warm. As the temperature reached  $145^\circ\text{K}$  there was again a sudden increase in both temperature and deposit reflectance, but the sudden reflectance increase was only about 6 percent (from 65 to 71 percent). This was considerably less than the jump observed in Fig. 4. After the sudden reflectance increase the reflectance continued to increase gradually up to about 83 percent in the same manner as shown for the deposit in Fig. 4. The small jump was due to the fact that most of the amorphous ice had already transformed to the cubic state.

The reflectance of the 4-mm water deposit after the system was pressurized, the chamber again evacuated, and the cryosurface temperature raised to  $200^\circ\text{K}$ , is shown in Fig. 12. The reflectance curve shapes and magnitude resemble that shown in Fig. 5, but

with some slight differences. The absorption bands at 1.04, 1.25, 1.55, 2.04, and around 3.0  $\mu$  appear for both cases. In Fig. 12 there is a peak in the reflectance at about 3.5  $\mu$  whereas no peak was observed for the deposits formed on the black substrate (Fig. 5). There was a difference in the experimental procedure used to arrive at the two reflectance spectra shown in Figs. 5 and 12 other than different substrates. The deposit for Fig. 5 was warmed up under vacuum. For the deposit of Fig. 12 the chamber was pressurized to atmosphere for about one hour, the surface allowed to warm up to 200°K, and then cooled back down to about 100°K. The main difference between the two experiments was the fact that the surface reflectance shown in Fig. 12 was obtained after the deposit had been exposed to a dry-nitrogen pressure of 740 torr and nitrogen gas was undoubtedly absorbed. It is interesting that the 3.5- $\mu$  peak should occur for this latter case and indicates that this peak was somehow related to the deposit being subjected to the dry nitrogen. No significant difference in the reflectance was seen for wavelengths slightly less or greater than 3.5  $\mu$ . It would appear that the reflectance peak at 3.5  $\mu$  was not attributable to scattering alone but was probably caused by the increased transmission in this region. This peak is present in reflectance data obtained by other investigators for water frosts formed at atmospheric pressure (Refs. 17 and 18), and also for experiments performed at this laboratory in which the frost was pumped directly from the atmosphere.

Although absorption bands were found to occur at the same wavelength for the different crystalline forms of water deposit, this was not unexpected. It has been pointed out previously (Ref. 12) that the major absorption bands for the hexagonal and cubic form of water occur at approximately the same wavelengths. Based on the results of the present study, this conclusion can also be extended to include amorphous ice.

The reflectance variation with deposit thickness is shown in Fig. 13 for wavelengths of 0.5, 1.01, 2.02, 4.10, and 8.05  $\mu$ . These reflectances are for the deposits whose spectral reflectances are shown in Fig. 11. The reflectance at 0.5  $\mu$  dropped from an initial value of 50 percent down to 30 percent and then was followed by a gradual rise back up to 46 percent at 4.0-mm thickness. This was almost back up to the initial value. For the other wavelengths, the reflectance was considerably less than the initial value regardless of the deposit thickness. The behavior of the 0.5- $\mu$  curve was explained earlier for carbon dioxide in Ref. 3. It was determined that the initial drop in reflectance was attributable to two effects: (1) the change in the relative refractive index at the stainless steel surface and (2) a further decrease that was attributable to radiation trapped in the deposit because of the critical angle effect. The latter effect was caused by radiation being scattered such that the rays were internally incident on the deposit surface at angles greater than the critical angle. This radiation was then totally reflected back to the substrate which increased the possibility of its being absorbed by the stainless steel.

## SECTION VI DISCUSSION

The reflectance of amorphous water deposits formed on polished stainless steel and black epoxy paint substrates has been presented in Figs. 3 through 13. As noted previously, these deposits can have an appreciable effect on the substrate thermal

radiative properties depending on the substrate reflectance, deposit thickness, wavelength, temperature, and pressure at which the deposits were formed.

The infrared reflectance of a black painted surface can be reduced to 1 percent or less which obviously is important in studies where background infrared radiation must be minimized. One application could be in infrared sensor tests where the wavelength range of interest is from 5 to 25  $\mu$ . In these tests the surroundings are black cryogenically cooled walls. By precoating the cold walls with a thin water deposit of from 50 to 100  $\mu$  thick, reflectances of 1 percent or less could be easily achieved provided that the deposit formed was amorphous. The vapor pressure of water deposits formed at these temperatures (77 and 4°K) is so low,  $< 10^{-24}$  torr, that migration to other cooled optical surfaces within the chamber would not be a problem. Although the reflectance of a surface could be greatly reduced by the presence of a thin layer of amorphous ice, a frost layer of the same thickness could cause an increase in the visible and near infrared reflectance. This increase could be an order of magnitude if the deposit formed was Ice Ih. Therefore, some care must be taken to form the deposit in the correct manner in order to achieve the desired results. This means that a "hot spot" on a cryogenically cooled panel could play havoc with any attempt to produce a very black surface. In some instances the formations of Ih or Ic at one spot have been seen to propagate across an amorphous deposit.

The effects of water deposits formed on polished stainless steel indicate that the presence of even very thin films of water on a cooled mirror can change the infrared reflective properties from highly reflecting to highly absorbing. As was pointed out earlier in Ref. 3, this reduction in reflectance is especially crucial in airborne applications which employ cooled optics. Whereas the possibility of contamination by carbon dioxide frosts will be small because of the relatively small abundance of carbon dioxide in the atmosphere, the contamination by thin water films on the other hand will be inevitable. Additionally, the highly absorbing feature of water deposits for wavelengths greater than about 1.5  $\mu$  will make the deposits even more troublesome in the infrared region as was shown by a deposit only 30  $\mu$  thick on the polished stainless steel surface. For any system requiring cooled optics, a concerted effort will have to be made to minimize the contamination of the optical surfaces by water.

In vacuum systems such as space simulation chambers, the water deposits can in general form in any of three different forms: Ih, Ic, and amorphous. The reflectance will largely depend on which of these three types or mixtures of these forms are obtained during deposition.

Previously, the phase changes of water were studied using calorimetric techniques and X-ray diffraction. The results shown in Fig. 4 are unique in that they show quantitatively the visual ( $\lambda = 0.55 \mu$ ) changes in reflectance during these phase changes. In Fig. 4 the reflectance change was from about 43 percent up to 66 percent which was easily observed visually. This disagrees with the findings of Ghormley (Ref. 19) who reported that no visual change could be detected for 5-mm-thick deposits during the transition. In the present study, the transition started at some point on the test surface and spread over the remainder of the surface within 10 to 15 sec. The transition from cubic to hexagonal on the other hand was gradual, and the appearance of the deposit

after it had transformed to hexagonal was much whiter than that for the cubic structure. As mentioned by several investigators, the point at which the temperature suddenly increases depends on the rate of warming. At the higher rates of warming, as in this study and in that of Pryde and Jones (Ref. 8), the transition temperature seems to be at  $145 \pm 2^\circ\text{K}$ . The dependence on the rate of warming is the probable cause for the wide variation in temperature from 110 to  $150^\circ\text{K}$  reported by various investigators for the amorphous to cubic transition.

## SECTION VII CONCLUDING REMARKS

The present investigation has presented in situ spectral absolute reflectance measurements of water deposits formed under vacuum conditions. The wavelength range covered was from 0.5 to  $12.0\ \mu$ . Water cryodeposits from 0.03 to 4.0 mm thick were formed on liquid-nitrogen-cooled surfaces and were found to appreciably affect the reflectance over the entire wavelength range. From this study, several observations on the effects of water deposits are made:

1. The reflectances of cold black surfaces can be reduced by coating them with a thin water, cryodeposited film. In particular, between 2 and  $12\ \mu$ , the reflectance can be reduced by a factor of 2 or 3 to 1 percent or less for a water deposit thickness of 50 to  $100\ \mu$ .
2. Water deposits formed on a polished stainless steel surface reduced the reflectances over the entire wavelength range. In the infrared, a deposit only  $30\ \mu$  thick reduced the reflectance from about 75 down to about 15 percent. This indicates that cooled optics can be seriously affected in the infrared.
3. The reflectance of a water cryodeposit is extremely sensitive to the temperature of the deposit or to the surface on which it is formed. All three forms of Ice I were observed; the amorphous, cubic (Ic), and hexagonal (Ih). The exothermic transition from the amorphous to cubic state was observed to occur at about  $145^\circ\text{K}$  ( $-128^\circ\text{C}$ ). Further temperature increase caused the deposit to transform to the hexagonal configuration. The reflectance of these deposits increased as the deposit changed from amorphous to Ic to Ih.
4. Weak absorption bands were found at 1.04 and  $1.25\ \mu$  and strong absorption bands at 1.55, 2.04, 3.0, and  $4.5\ \mu$ . A broad region of strong absorption was observed for wavelengths between 3 and  $12\ \mu$  with it being impossible to pick out a narrow absorption band in this region. The region of strongest absorption appeared to be between 3 and  $7\ \mu$ . All absorption bands apparently occurred in the same regions for Ih and amorphous ice.
5. A small anomalous dispersion peak was observed in the reflectance of water on black paint between 3.1 and  $3.25\ \mu$ . As explained in Ref. 3,

this was caused by the high reflectance associated with a strong absorption band and was caused by a rapid increase in the refractive index as the absorption band was approached.

6. For one experiment a peak in the reflectance curve was seen at 3.5 to 3.7  $\mu$  for a 4-mm-thick water deposit formed on stainless steel. This was after the deposit had been formed under vacuum and then exposed to dry nitrogen gas at 740-torr pressure. Broad peaks in the reflectance were also sometimes seen in the region of 9.5  $\mu$ .

The reflectances of the water frosts are of general interest with regard to: (1) studies of thermal radiative properties in simulation chambers with cryogenically cooled surfaces, (2) any experimental apparatus requiring cryogenically cooled mirrors, windows or lenses, (3) studies involving planetary frosts, (4) effects of thin deposits formed on low temperature blackbodies which are used as calibration standards, and (5) comparison with analytical results obtained from reflectance models for absorbing and scattering media.

#### REFERENCES

1. Dorsey, N.E. Properties of Ordinary Water-Substance in All of Its Phases. Reinhold Publishing Corporation, 1940, p. 395.
2. McCullough, B.A., Wood, B.E., Smith, A.M., and Birkebak, R.C. "A Vacuum Integrating Sphere for In Situ Reflectance Measurements at 77°K from 0.5 to 10 Microns." Progress in Astronautics and Aeronautics. Academic Press, Inc., Vol. 20, 1967, p. 137.
3. Wood, B.E., Smith, A.M., Seiber, B.A., and Roux, J.A. "Infrared Reflectance of CO<sub>2</sub> Cryodeposits." AEDC-TR-70-108, July 1970.
4. Wood, B.E. and Smith, A.M. "Spectral Reflectance of Water and Carbon Dioxide Cryodeposits from 0.36 to 1.15 Microns." AIAA Journal, Vol. 6, No. 7, 1968, pp. 1362-1367.
5. Eisenberg, D. and Kauzmann, W. The Structure and Properties of Water, Clarendon Press, 1969, p. 71.
6. Sugisaki, M., Suga, H., and Seki, S. "Calorimetric Study of Glass Transition of the Amorphous Ice and of the Phase Transformation Between the Cubic and the Hexagonal Ices." Physics of Ice, Plenum Press, 1969, p. 329.
7. Dowell, L.G. and Rinfret, A.P. "Low Temperature Forms of Ice as Studied by X-Ray Diffraction." Nature, Vol. 188, 1960, pp. 1144-1148.
8. Pryde, J.A. and Jones, G.O. "Properties of Vitreous Water." Nature, Vol. 170, 1952, pp. 685-688.

9. Burton, E.F. and Oliver, W.F. "The Crystal Structure of Ice at Low Temperatures." Proceedings of the Royal Society of London, Vol. 153 (Series A), 1936, pp. 166-172.
10. Bertie, J.E., Calvert, L.D., and Whalley, E. "Transformations of Ice II, Ice III and Ice V at Atmospheric Pressure." The Journal of Chemical Physics, Vol. 38, No. 4, 1963, p. 845.
11. Ockman, N. "The Infrared and Raman Spectra of Ice." Advances in Physics, Vol. 7, 1958, p. 199.
12. Bertie, J.E. and Whalley, E. "Infrared Spectra of Ices Ih and Ic in the Range 4000 to 350  $\text{cm}^{-1}$ ." Journal of Chemical Physics, Vol. 40, No. 6, March 1964, pp. 1637-1645.
13. Hornig, D.F., White, H.F., and Reding, F.P. "The Infrared Spectra of Crystalline  $\text{H}_2\text{O}$ ,  $\text{D}_2\text{O}$ , and  $\text{HDO}$ ." Spectrochimica Acta, Vol. 12, 1958, pp. 338-349.
14. Kieffer, H. "Spectral Reflectance of  $\text{CO}_2\text{-H}_2\text{O}$  Frosts." Journal of Geophysical Research, Vol. 75, No. 3, 1970, pp. 501-509.
15. Müller, P.R. "Measurements of Refractive Index, Density, and Reflected Light Distribution for Carbon Dioxide and Water Cryodeposits and also Roughened Glass Surfaces." PhD Thesis, University of Tennessee Space Institute, Tullahoma, Tennessee, 1969.
16. Beaumont, R.H., Chihara, H., and Morrison, J.A. "Transitions between Different Forms of Ice." Journal of Chemical Physics, Vol. 34, 1961, p. 1456.
17. Zander, R. "Spectral Scattering Properties of Ice Clouds and Hoarfrost." Journal of Geophysical Research, Vol. 71, No. 2, 1966, p. 375.
18. Keegan, H.J. and Weidner, V.R. "Infrared Spectral Reflectance of Frost." Journal of the Optical Society of America, Vol. 56, 1966, p. 523.
19. Ghormley, J.A. "Enthalpy Changes and Heat-Capacity Changes in the Transformations from High-Surface-Area Amorphous Ice to Stable Hexagonal Ice." The Journal of Chemical Physics, Vol. 48, No. 1, 1968, pp. 503-508.

**APPENDIX  
ILLUSTRATIONS**

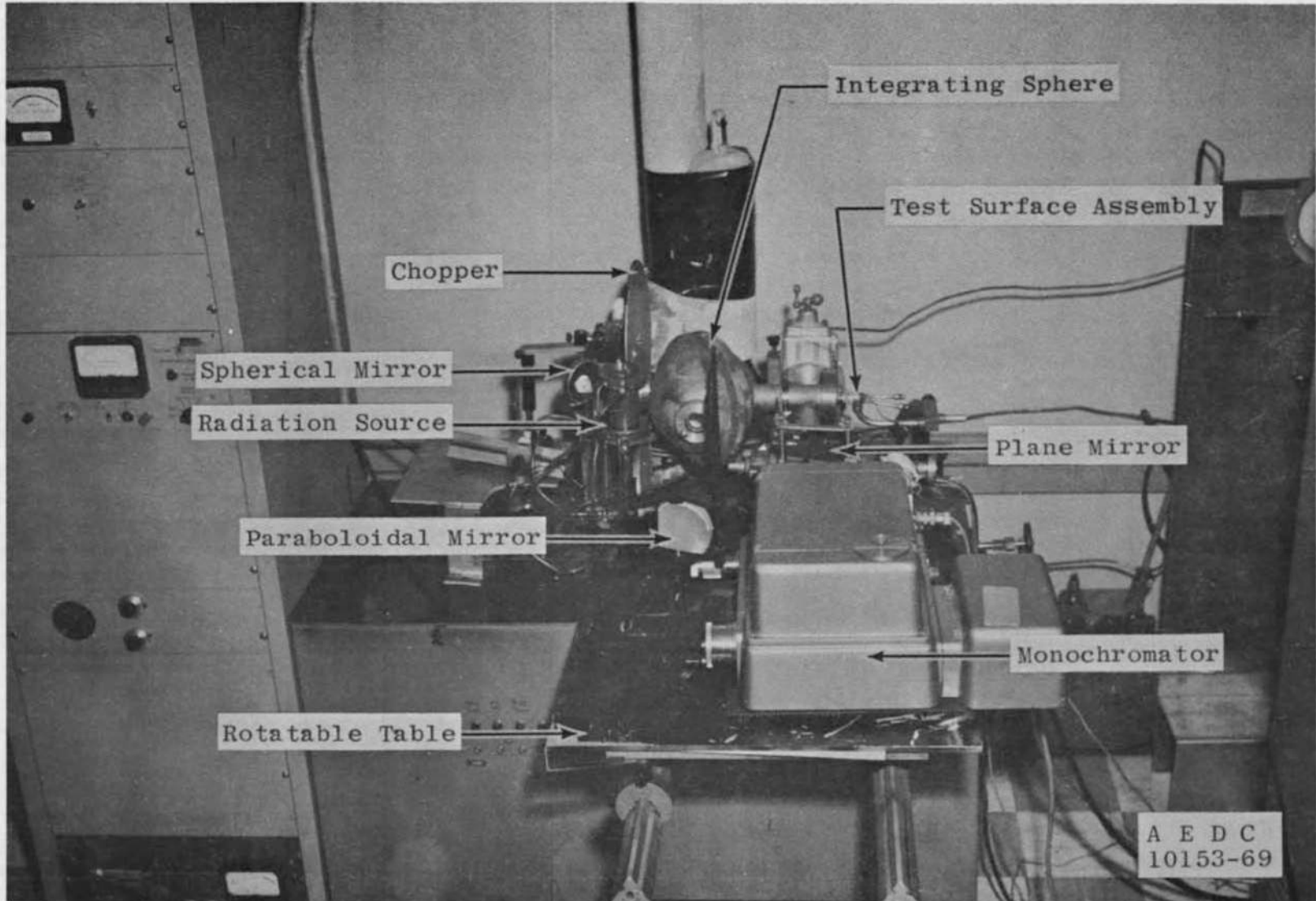


Fig. 1 Infrared Integrating Sphere and Optical Systems

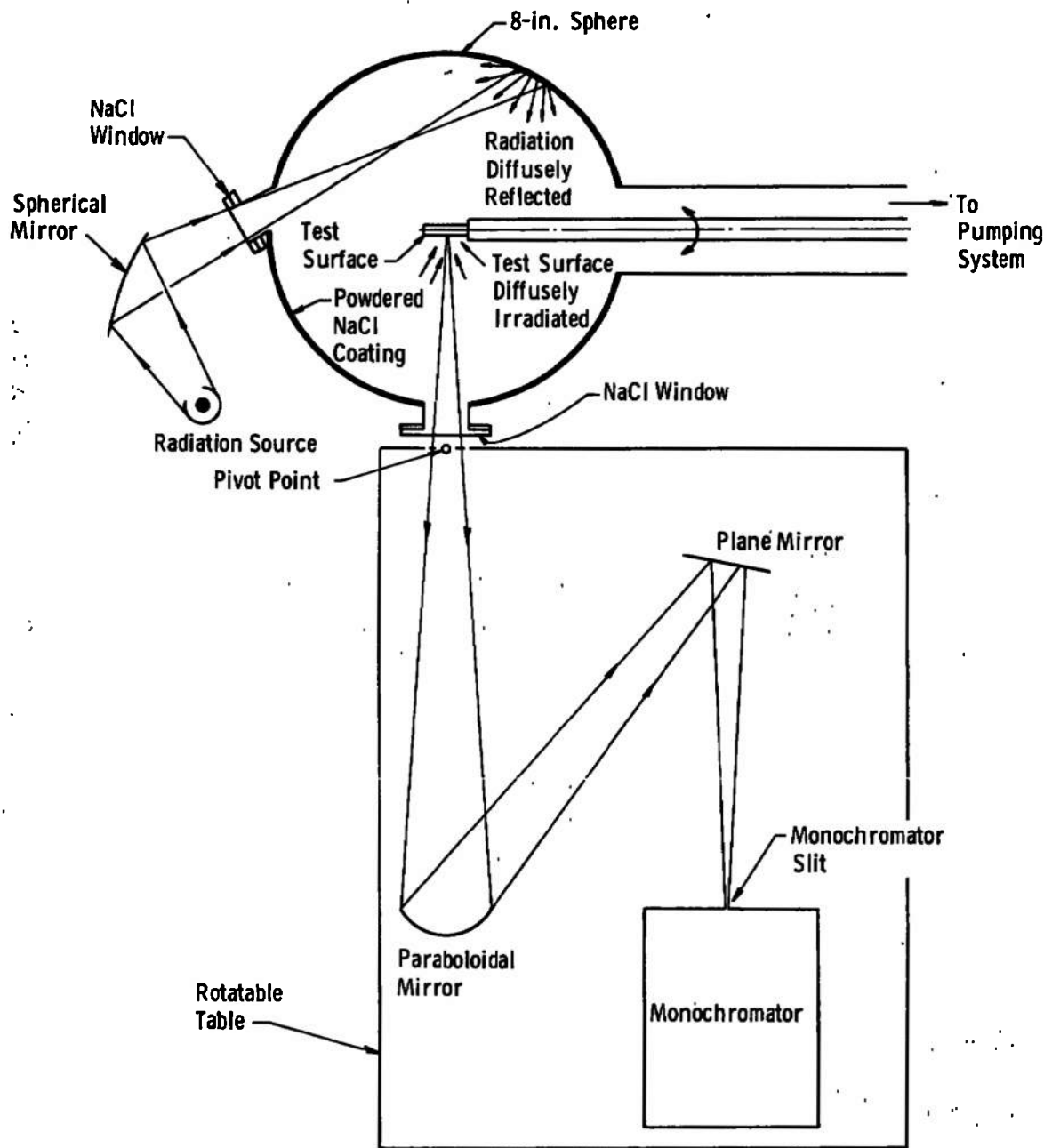


Fig. 2 Schematic of Infrared Integrating Sphere and Components

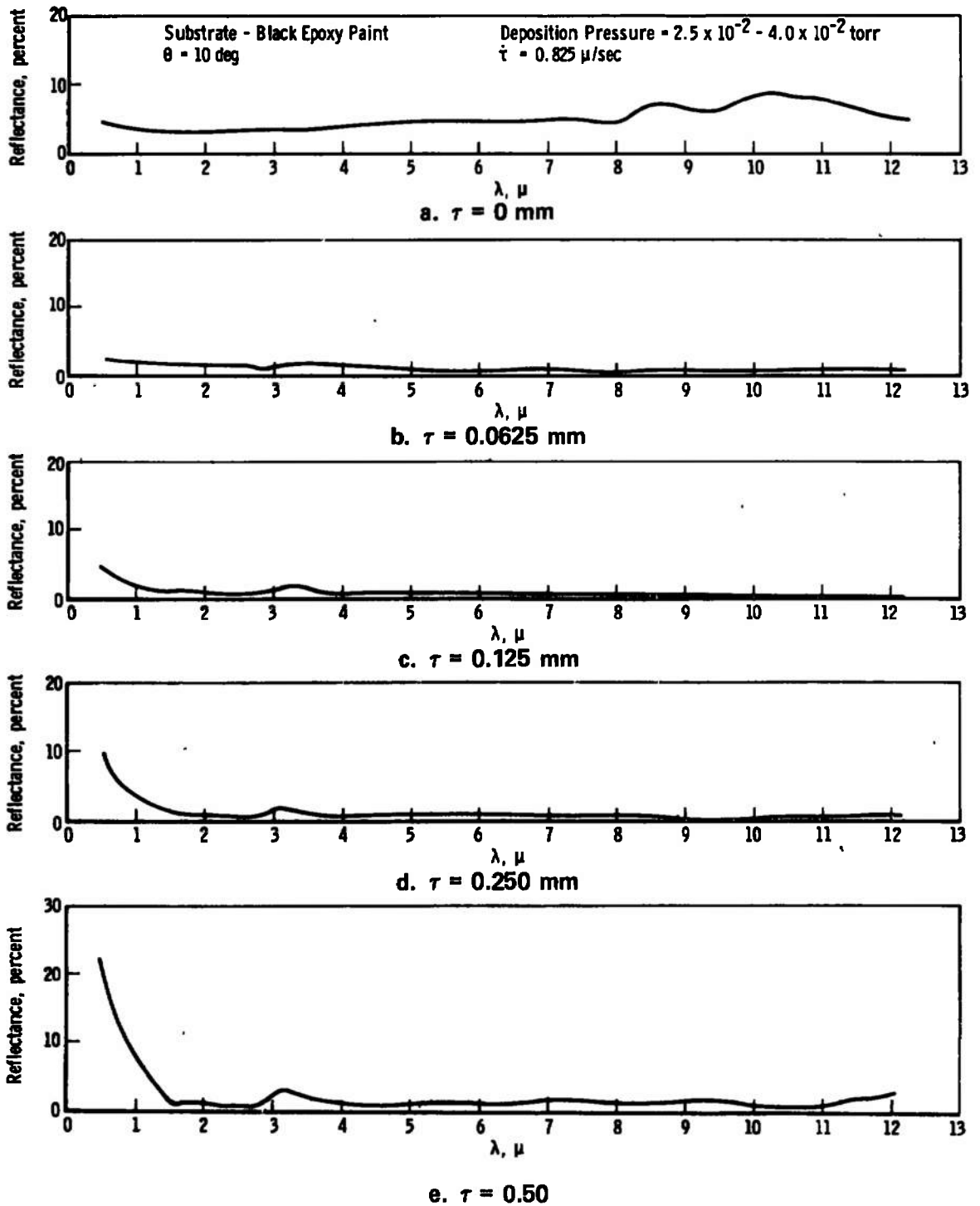
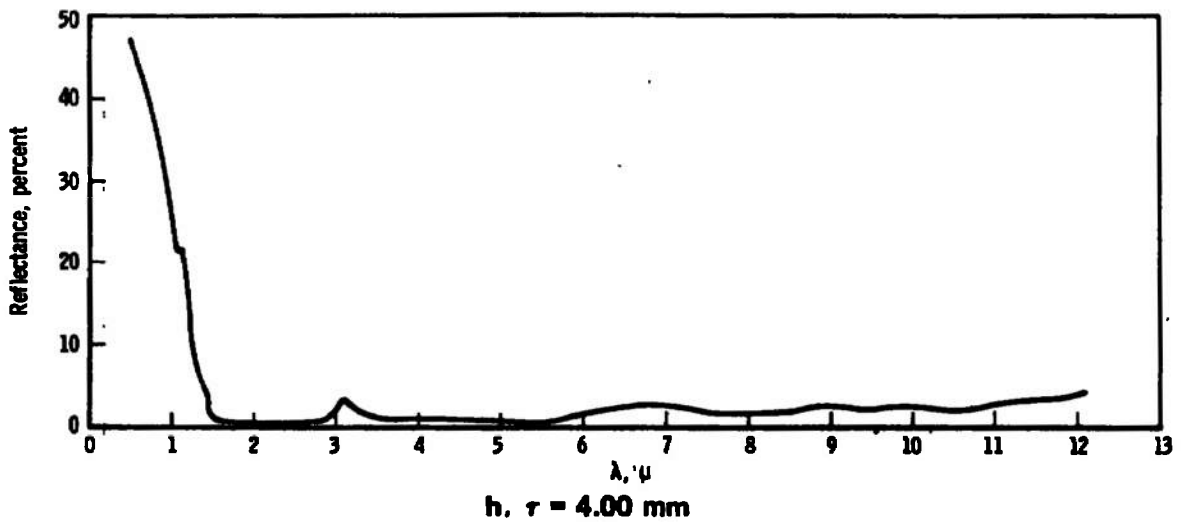
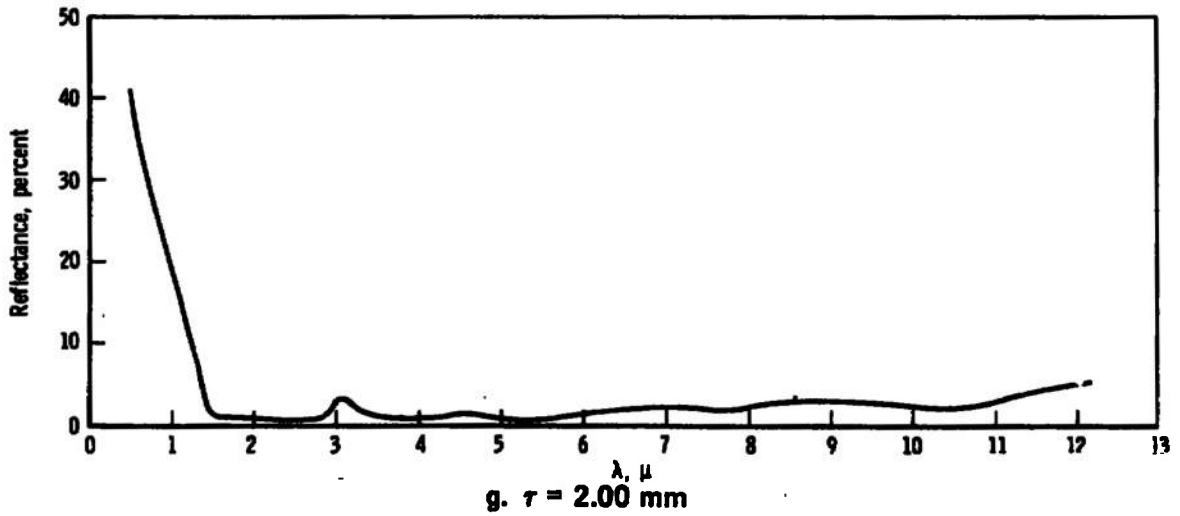
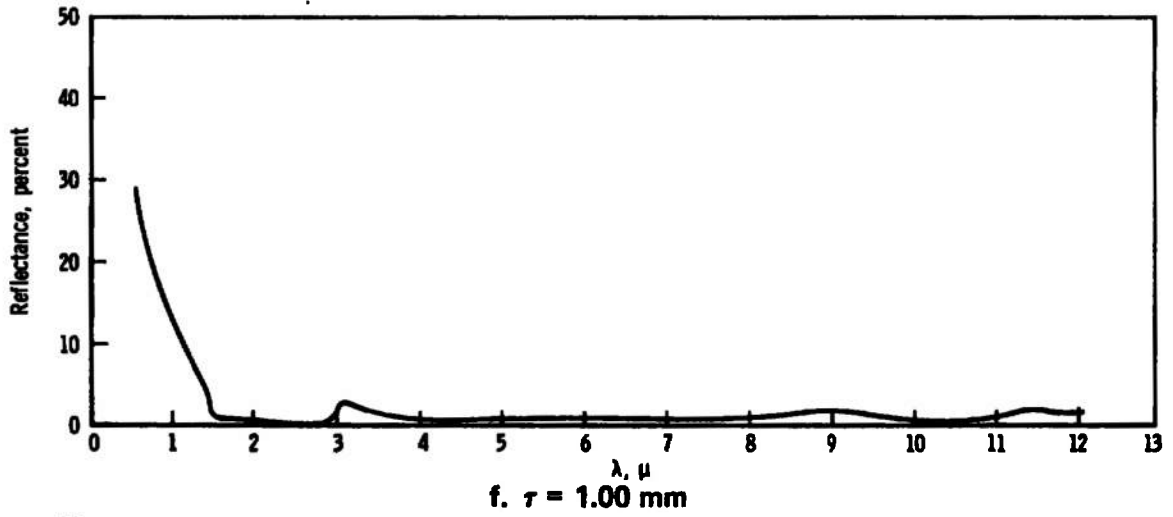


Fig. 3 Spectral Reflectance of Water Cryodeposits Formed on a Black Epoxy Painted Substrate



h.  $\tau = 4.00$  mm

Fig. 3 Concluded

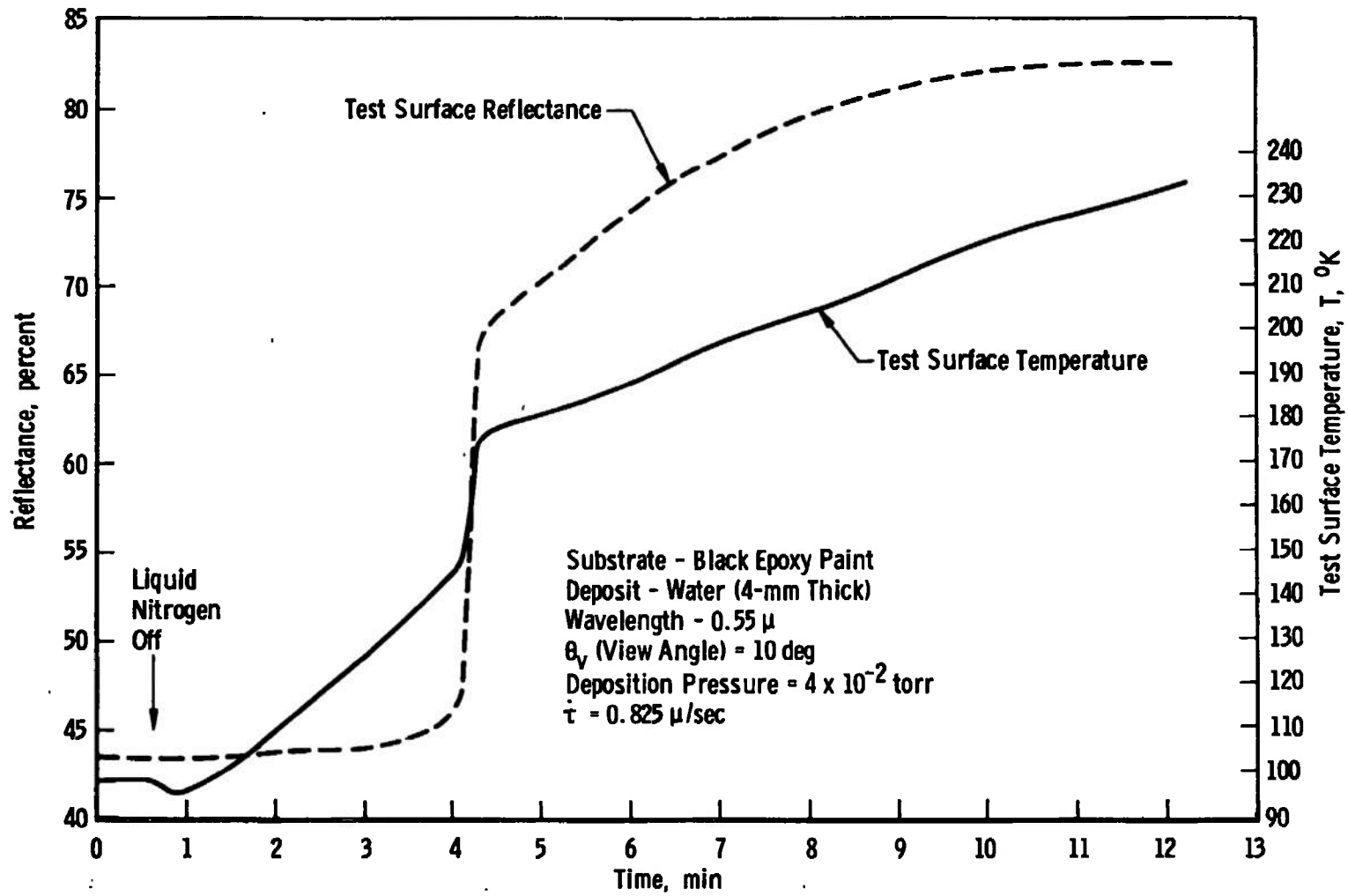


Fig. 4 Reflectance and Temperature Profile of Water Cryodeposit during Warmup

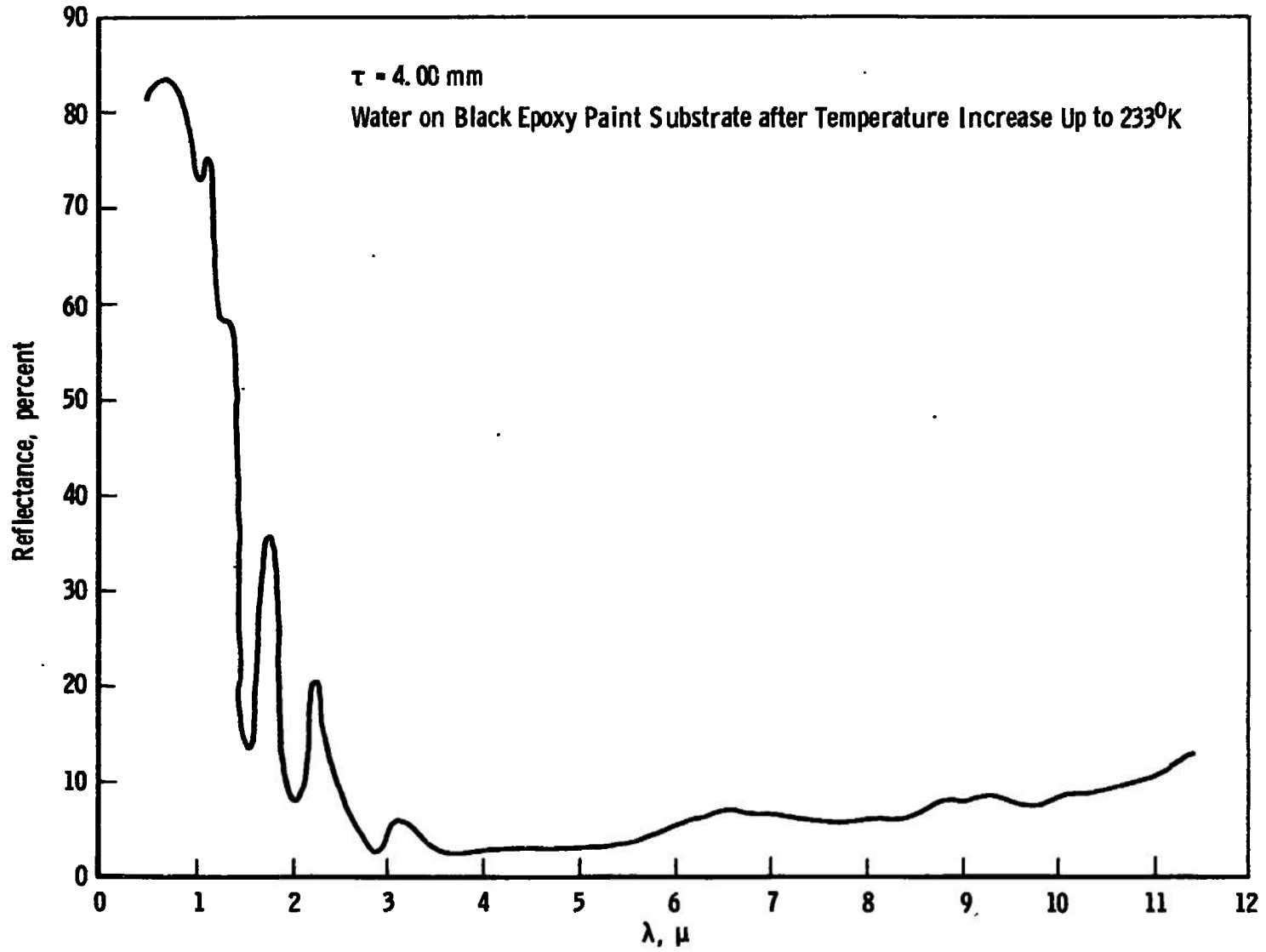


Fig. 5 Comparison of Reflectances of a 4-mm Water Deposit before and after Warmup

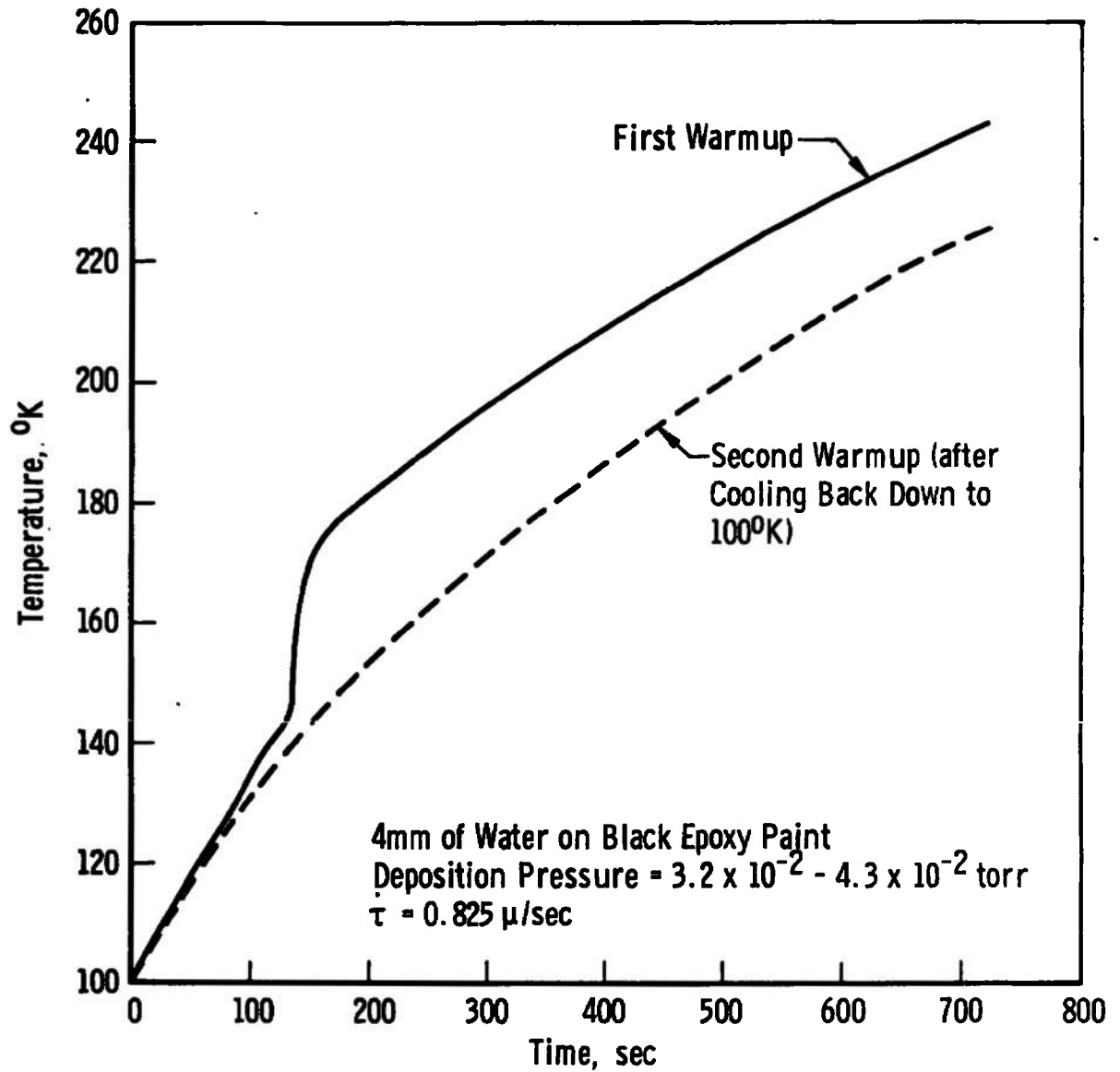
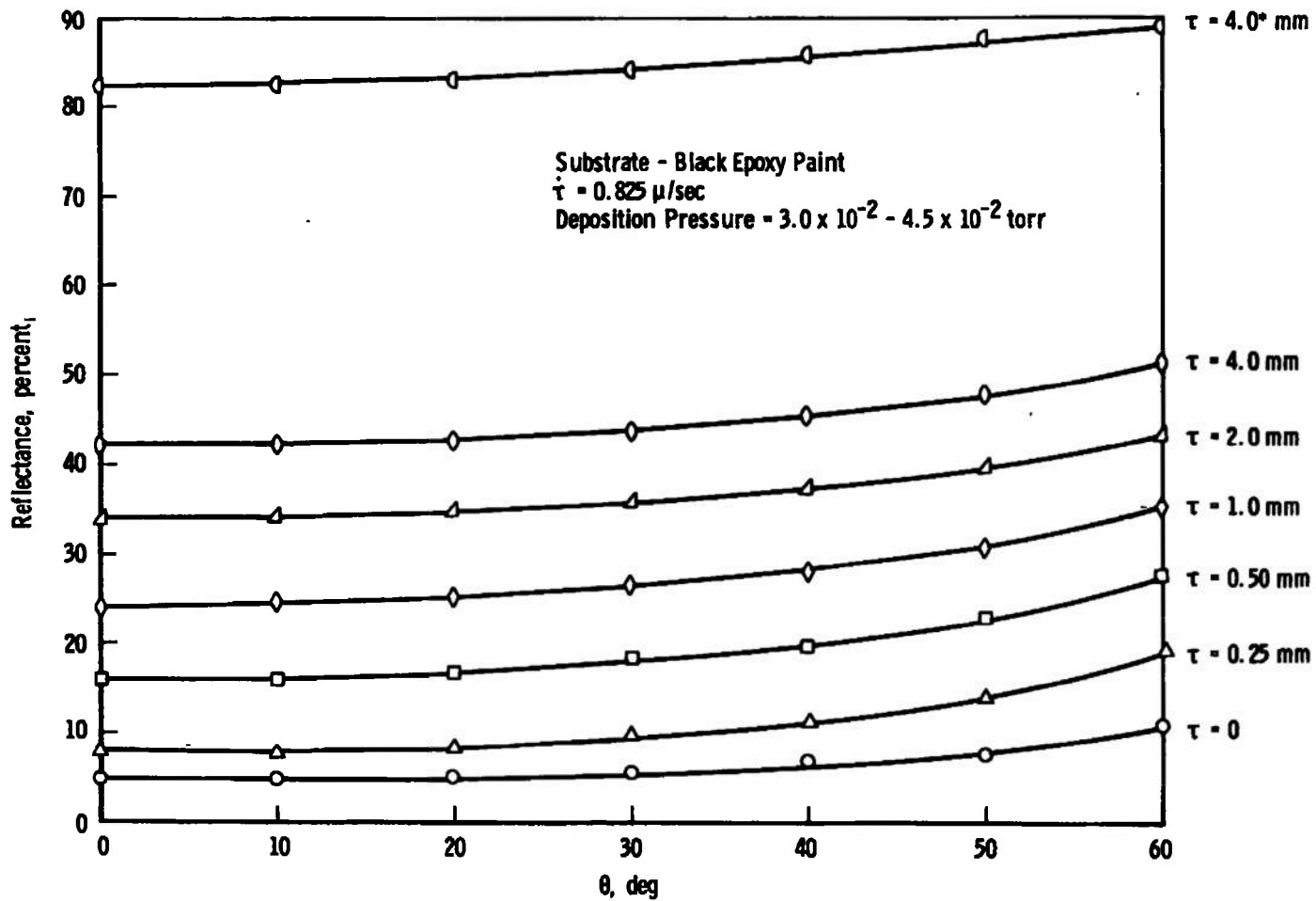
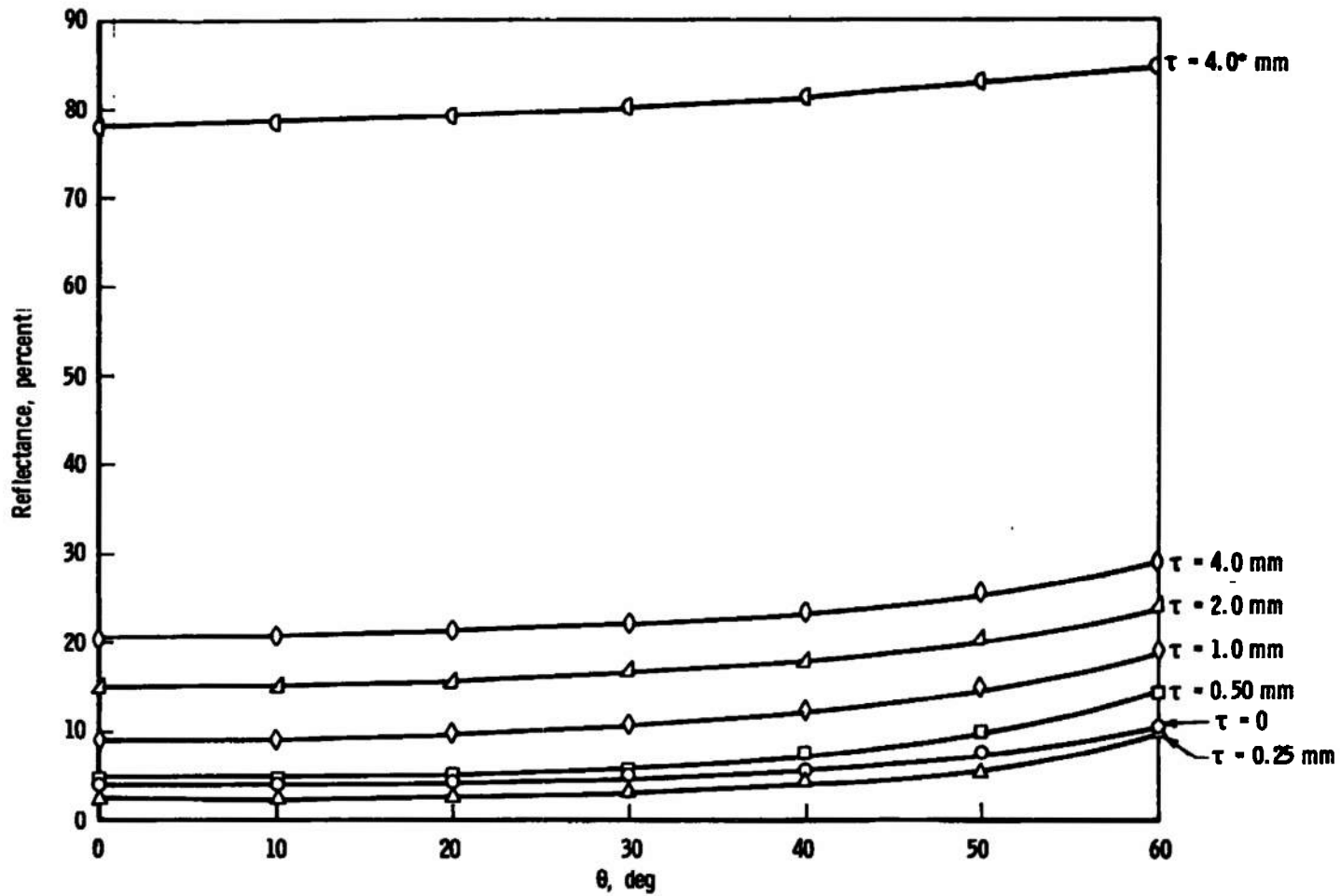


Fig. 6 Temperature versus Time Plot of a Water Deposit before and after Warmup

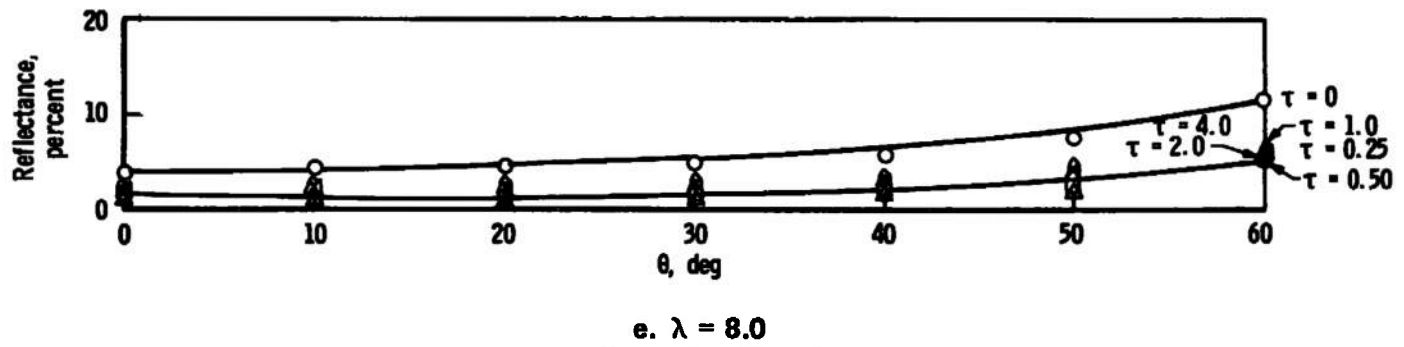
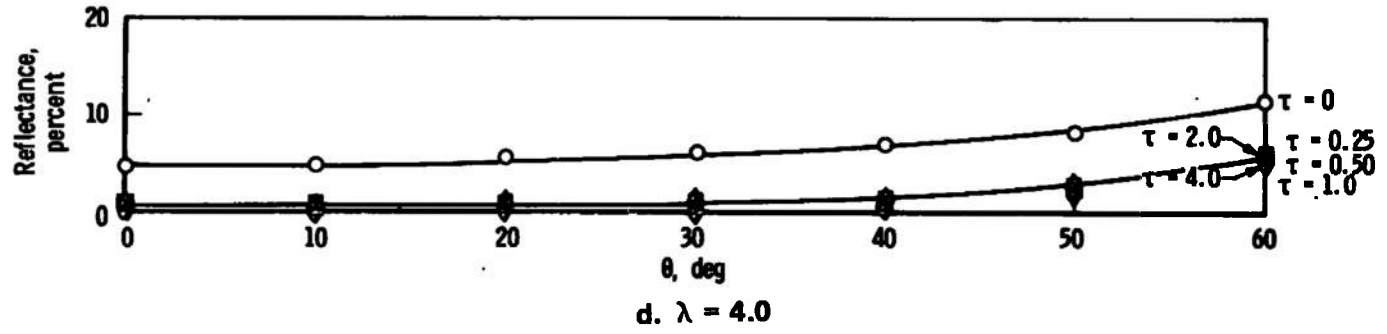
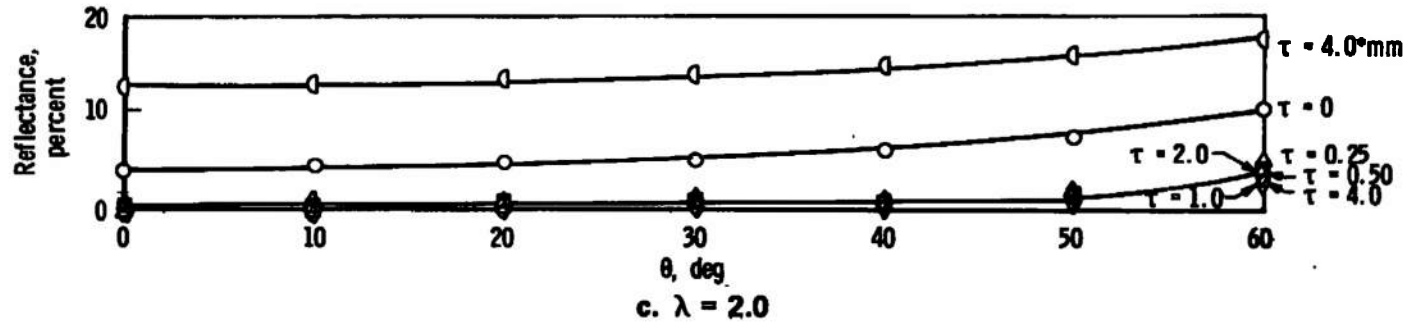


a.  $\lambda = 0.5$

Fig. 7 Dependence of Reflectance on View Angle,  $\theta$ , for Water Deposits Formed on a Black Epoxy Painted Substrate



b.  $\lambda = 1.0$   
Fig. 7 Continued



e.  $\lambda = 8.0$   
Fig. 7 Concluded

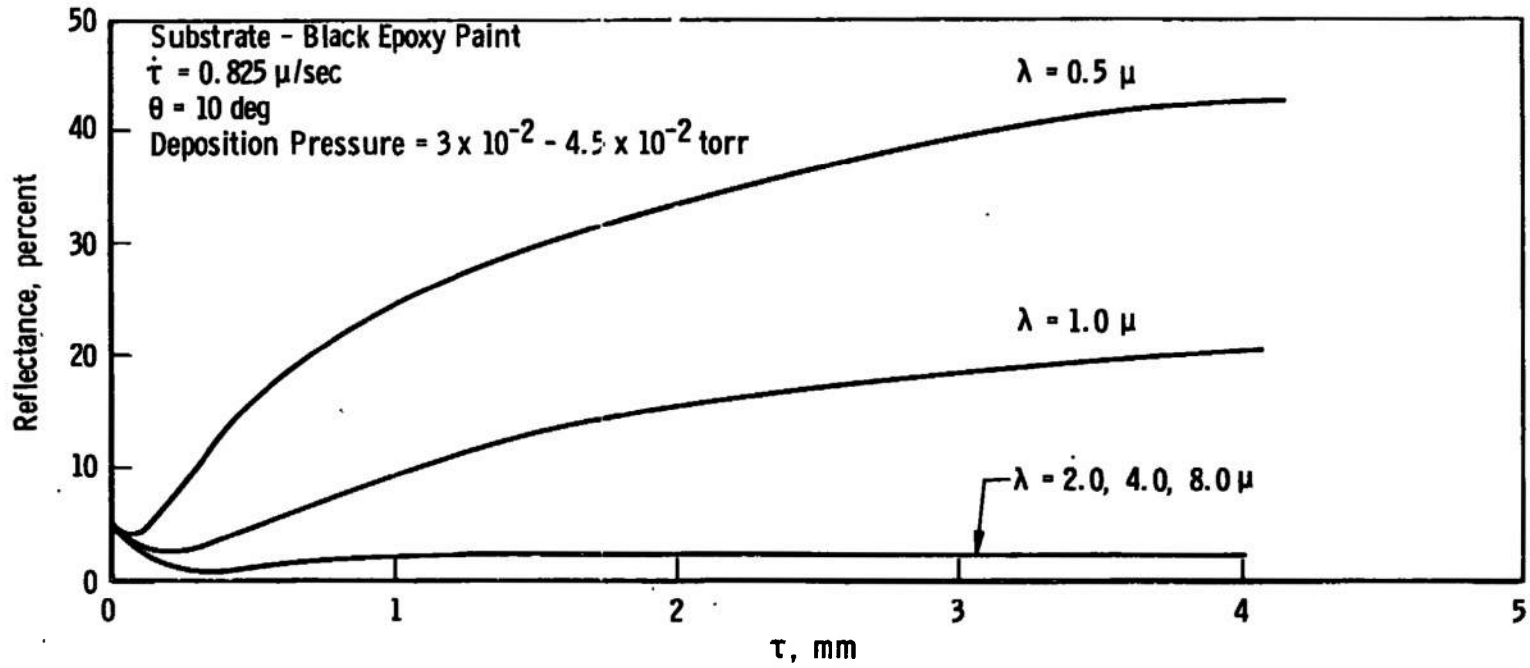


Fig. 8 Dependence of Reflectance on Deposit Thickness for Water Deposits Formed on a Black Epoxy Painted Substrate

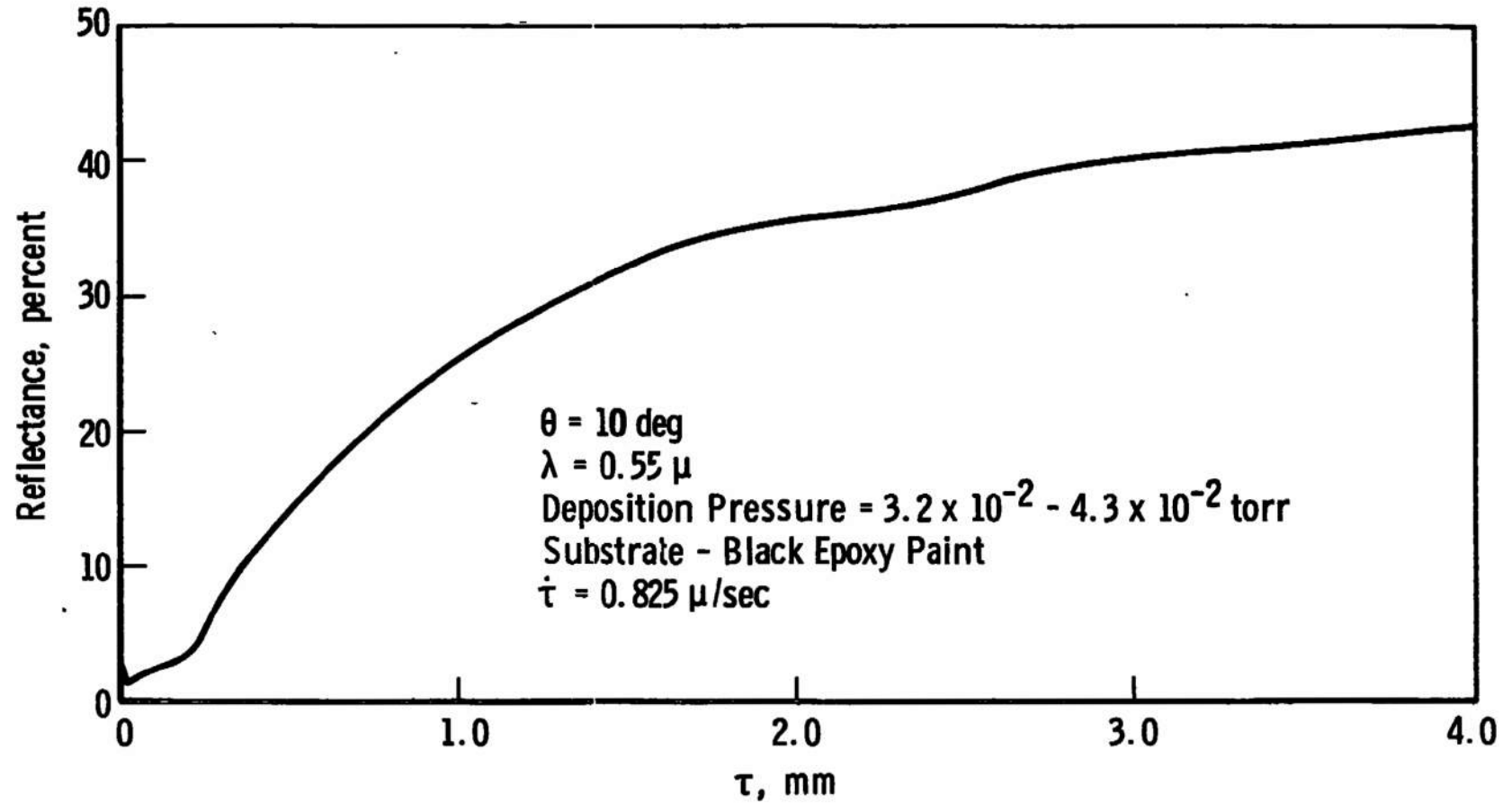


Fig. 9 Reflectance versus Thickness of a Water Deposit Formed Continuously on a Black Epoxy Painted Substrate for  $\lambda = 0.55 \mu$

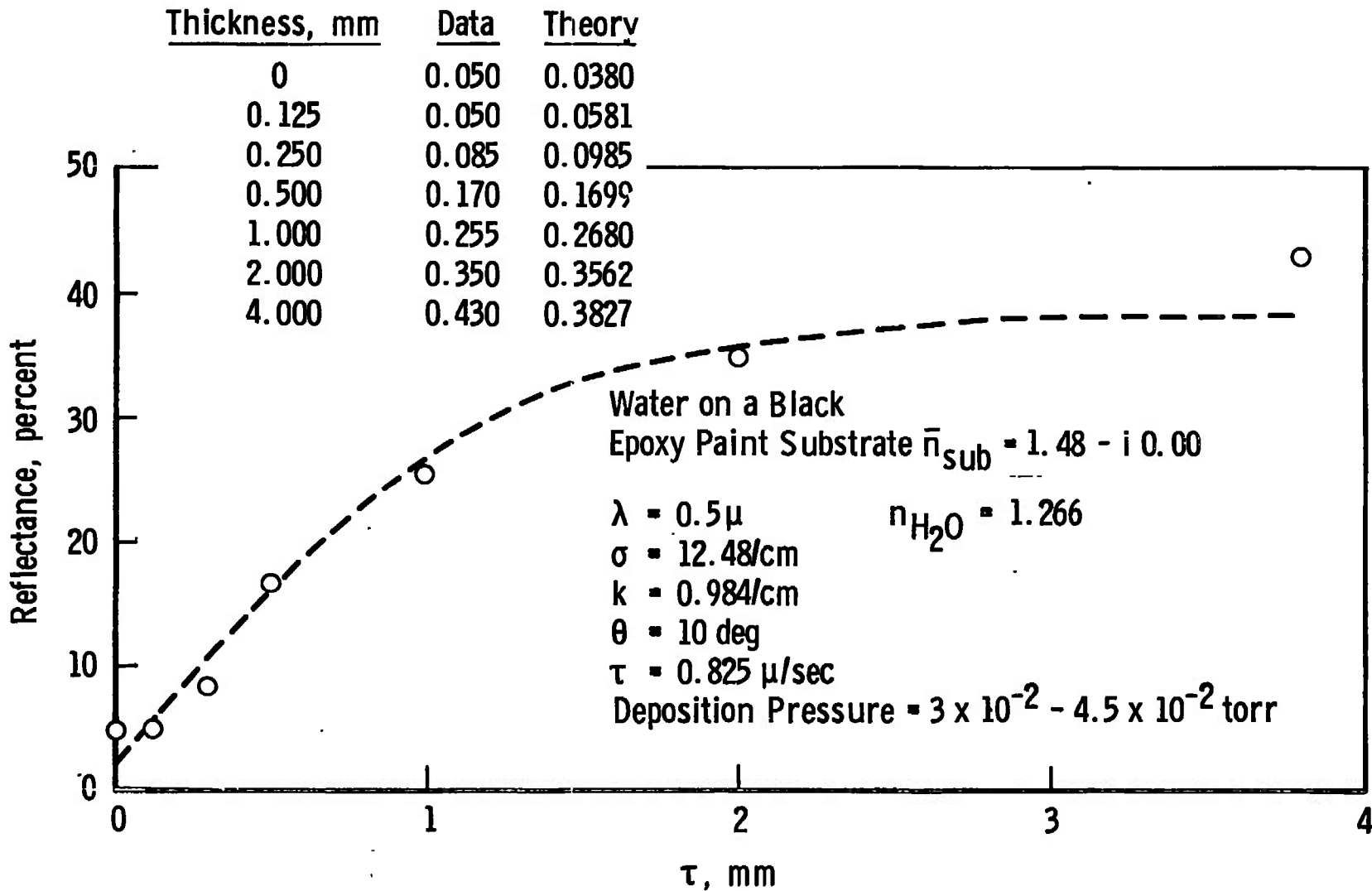
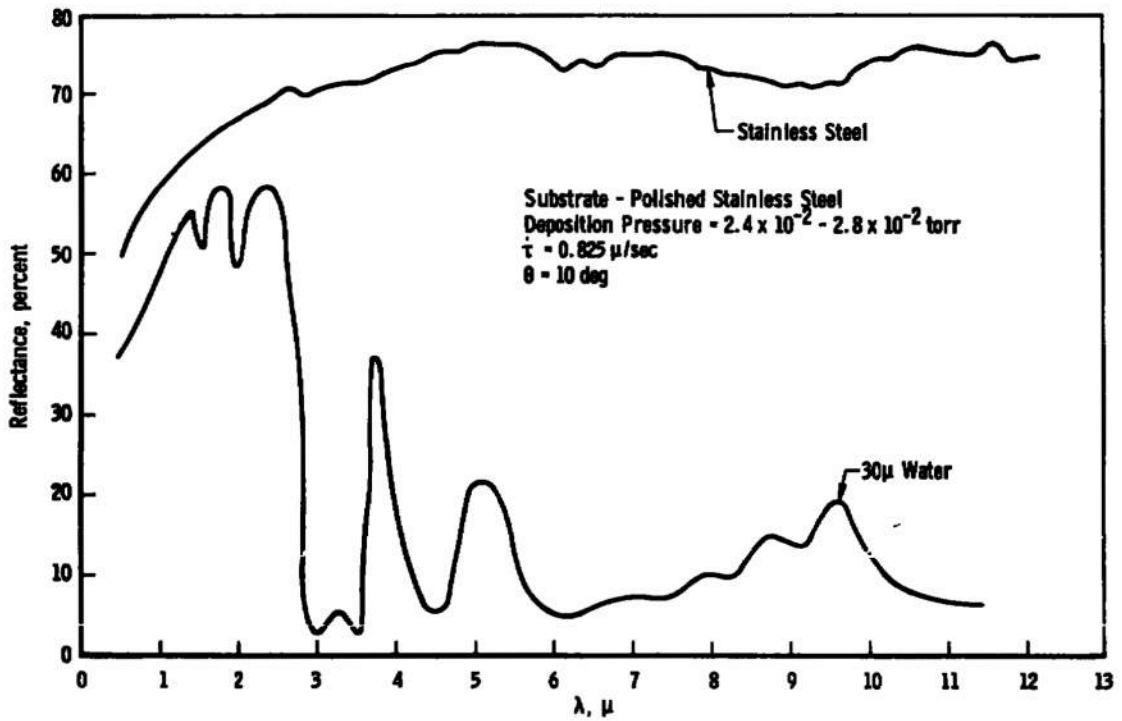
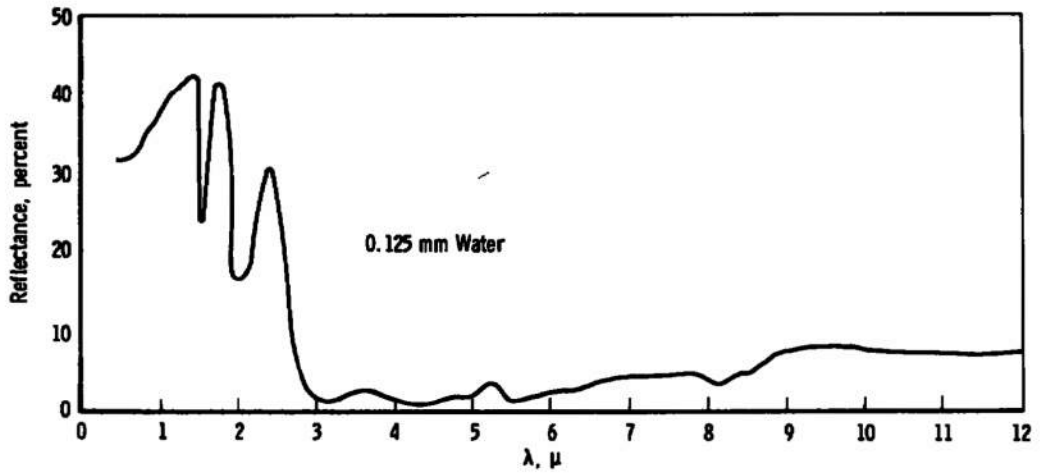


Fig. 10 Comparison of Experimental and Analytical Results for Reflectance versus Thickness of Water Deposits Formed on a Black Epoxy Painted Substrate

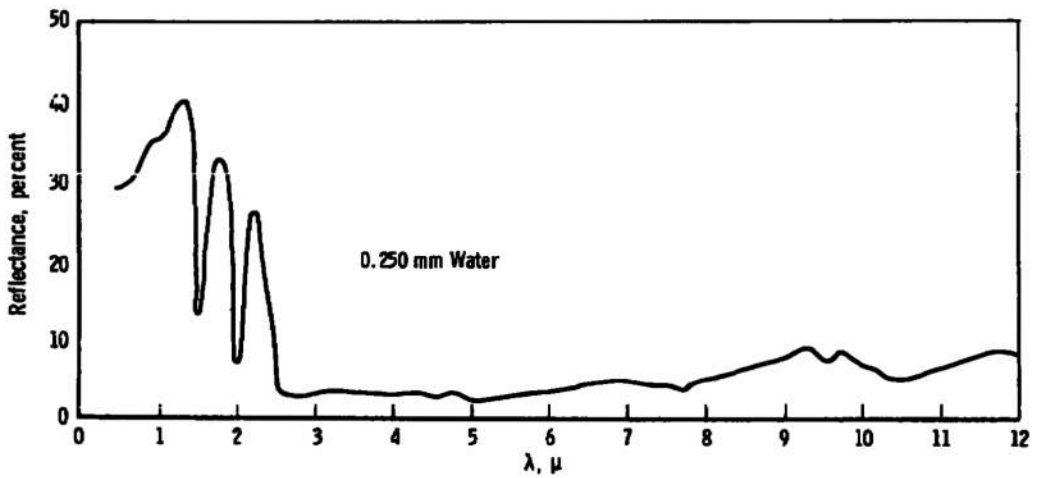


a.  $\tau = 30 \mu$

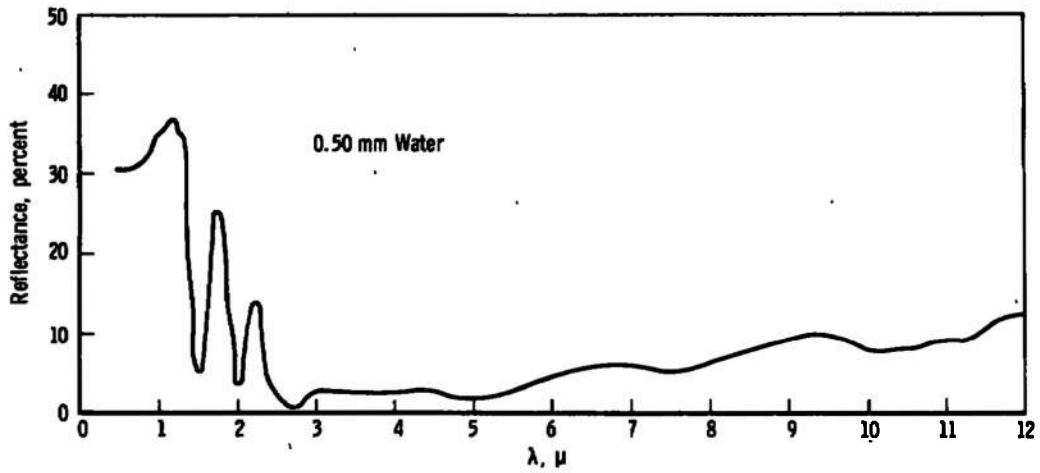
Fig. 11 Spectral Reflectance of Water Cryodeposits Formed on a Polished Stainless Steel Substrate



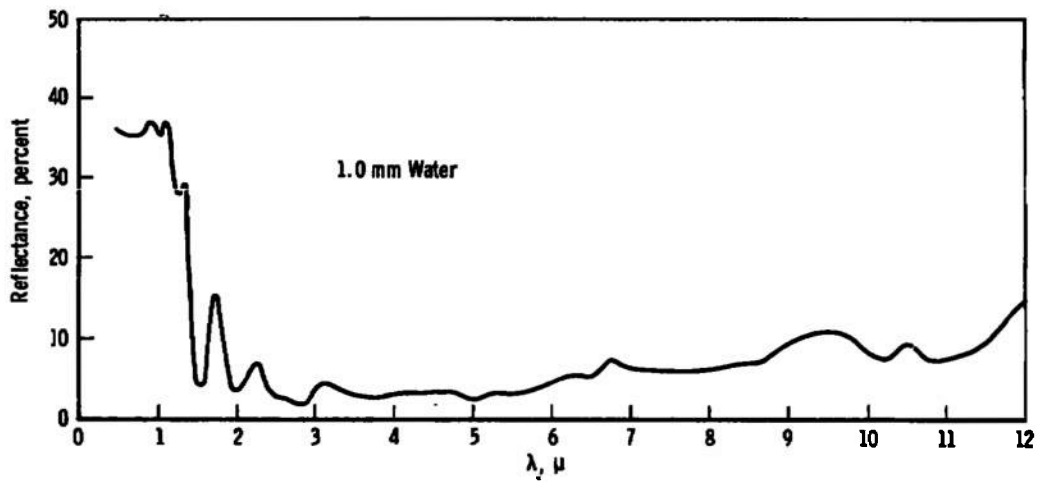
b.  $\tau = 0.125$  mm



c.  $\tau = 0.25$  mm  
 Fig. 11 Continued

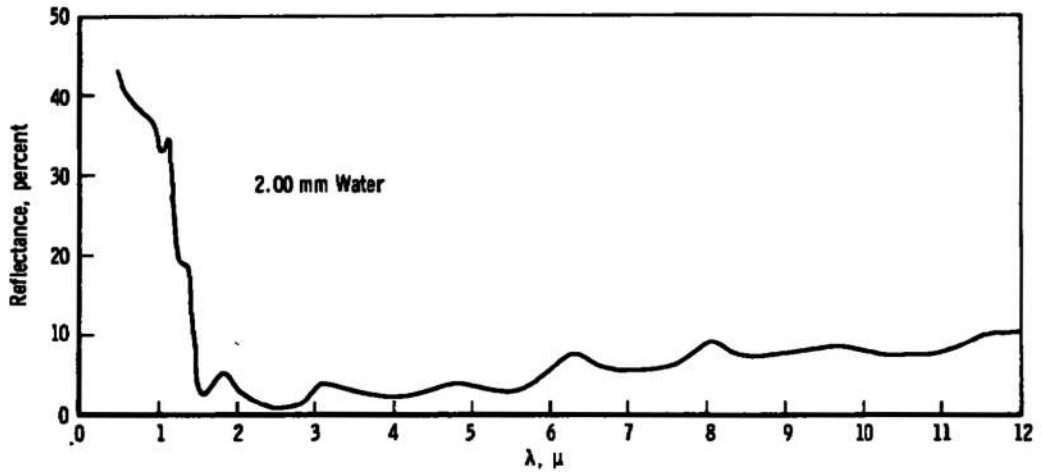


d.  $\tau = 0.50$  mm

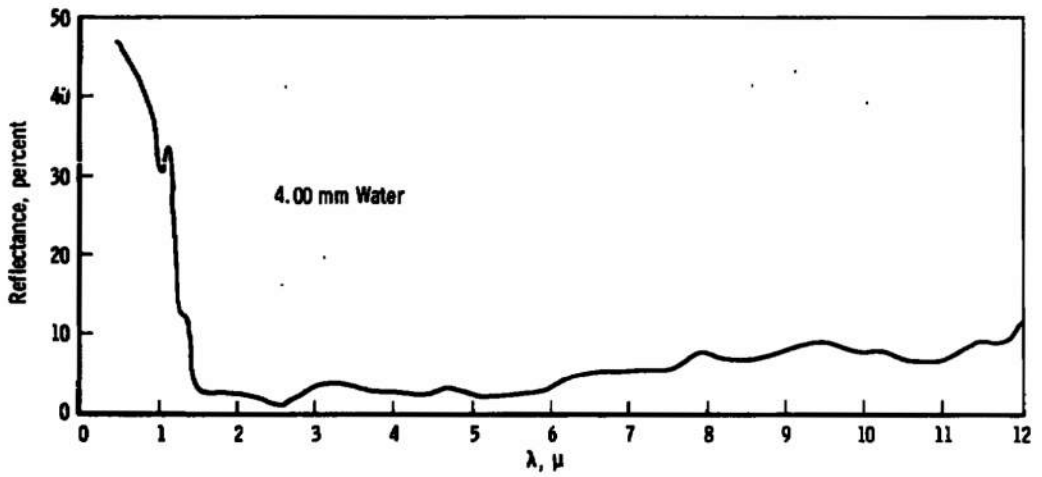


e.  $\tau = 1.0$  mm

Fig. 11 Continued



f.  $\tau = 2.00$  mm



g.  $\tau = 4.00$  mm

Fig. 11 Concluded

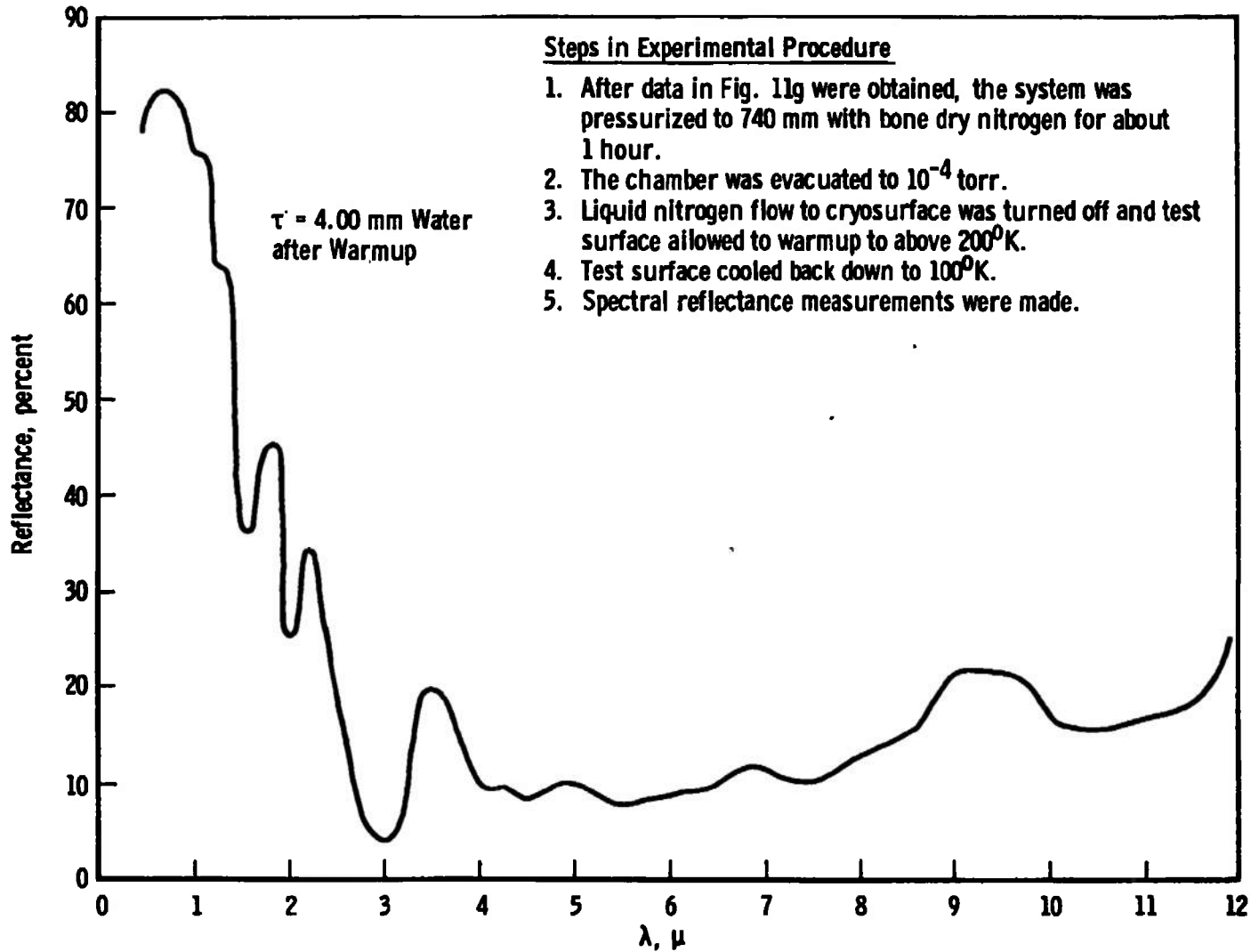


**Fig. 12 Comparison of Reflectances of a 4-mm Water Deposit on Stainless Steel before and after Warmup**

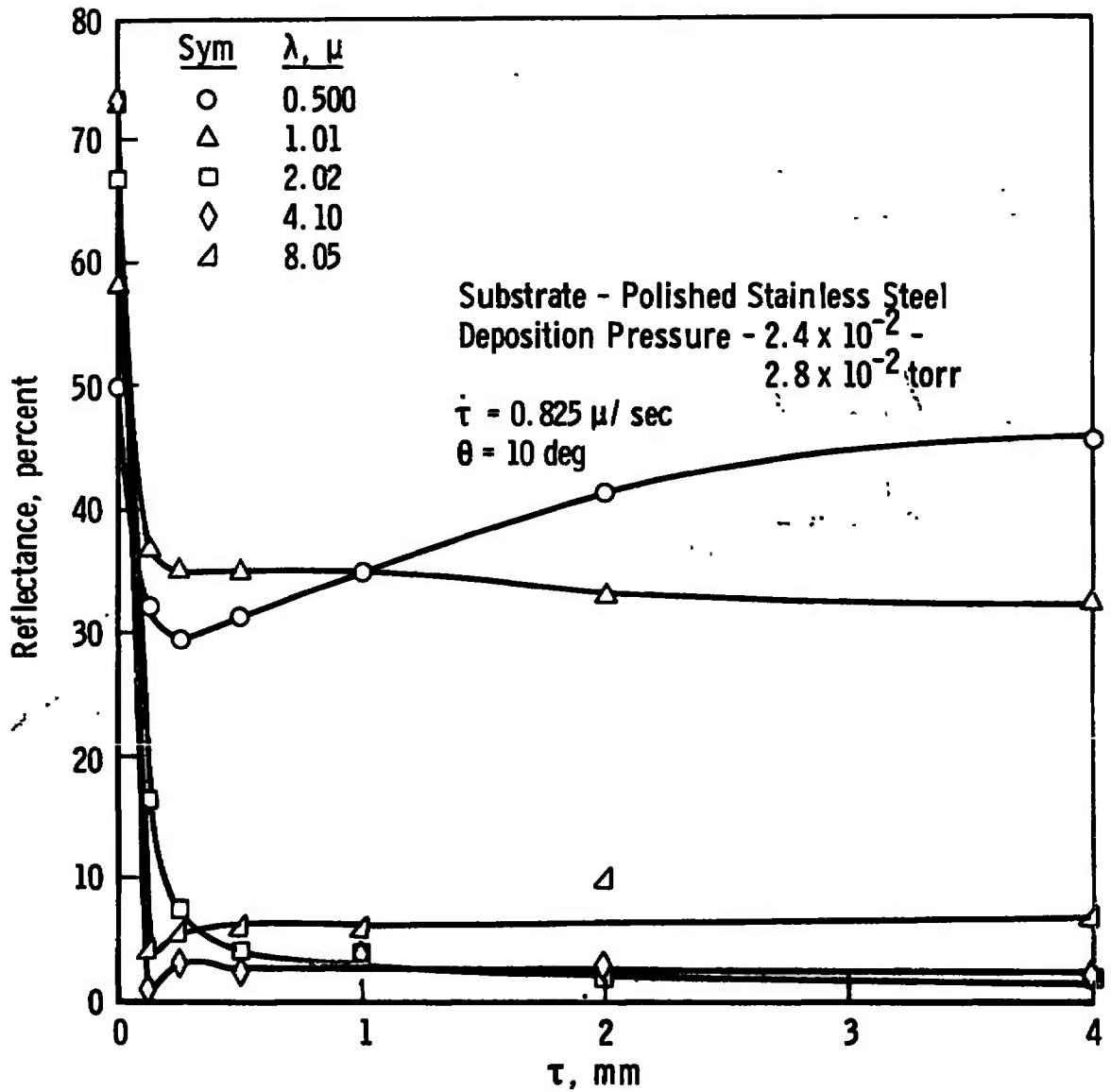


Fig. 13 Reflectance versus Thickness of Water Cryodeposits Formed on a Polished Stainless Steel Substrate

## DOCUMENT CONTROL DATA - R &amp; D

(Security classification of title, body of abstract and indexing annotation must be entered when the overall report is classified)

1. ORIGINATING ACTIVITY (Corporate author) Arnold Engineering Development Center ARO, Inc., Operating Contractor Arnold Air Force Station, Tennessee		2a. REPORT SECURITY CLASSIFICATION UNCLASSIFIED	
		2b. GROUP N/A	
3. REPORT TITLE INFRARED REFLECTANCE OF WATER FROSTS CONDENSED ON LIQUID-NITROGEN-COOLED SURFACES IN VACUUM			
4. DESCRIPTIVE NOTES (Type of report and inclusive dates) Final Report - July 1968 and September 1969			
5. AUTHOR(S) (First name, middle initial, last name) B. E. Wood, A. M. Smith, and B. A. Seiber, ARO, Inc., and J. A. Roux, University of Tennessee Space Institute			
6. REPORT DATE December 1970	7a. TOTAL NO. OF PAGES 41	7b. NO. OF REFS 19	
8a. CONTRACT OR GRANT NO. F40600-71-C-0002	8b. ORIGINATOR'S REPORT NUMBER(S) AEDC-TR-70-215		
b. PROJECT NO. 8951	9b. OTHER REPORT NO(S) (Any other numbers that may be assigned this report) ARO-VKF-TR-70-205		
c. Program Element 61102F			
d.			
10. DISTRIBUTION STATEMENT This document has been approved for public release and sale; its distribution is unlimited.			
11. SUPPLEMENTARY NOTES Available in DDC		12. SPONSORING MILITARY ACTIVITY Arnold Engineering Development Center, Air Force Systems Command Arnold AF Station, Tennessee 37389	
13. ABSTRACT Spectral absolute reflectance measurements from 0.5 to 12.0 $\mu$ were made for water cryodeposits formed on liquid-nitrogen-cooled surfaces in a vacuum infrared integrating sphere. The results are presented as functions of view angle, deposit thickness, and wavelength. The deposits were formed at pressures between $2 \times 10^{-2}$ and $4 \times 10^{-2}$ torr on cryogenically cooled black epoxy paint and polished stainless steel surfaces. All three forms of Ice I were observed - hexagonal, cubic, and amorphous or vitreous - and depended on the cryosurface temperature. The temperature of the deposit was found to play a strong role in determining the reflectance of any water deposit. From the results obtained in this investigation, important conclusions are drawn with regard to effects on space simulation and component studies in ground test facilities.			

14. KEY WORDS	LINK A		LINK B		LINK C	
	ROLE	WT	ROLE	WT	ROLE	WT
space simulation cryogenics cryopumping albedo spectral emittance ice (formation) dispersion infrared -- Reflectance crystallization  3. Frost 3 Ice -- Infrared reflectance						